A SYSTEM FOR THE COMPUTATION OF THE PHASE OF NETWORK FUNCTIONS BY THE COMPLEX - PLANE SCANNER.

A Report

Presented To

The National Research Council of Canada

Under Research Grant (A 584)

and

Bursary File No. (1-13-19-W-320)

by:

Helmut F. J. Wagerer

September, 1959.

ABSTRACT

This thesis discusses a system for the computation of phase slope and phase of network functions. The system is part of the complex-plane scanner, a special type of electronic analog computer, in which complex frequencies or vectors in the complex plane are represented by sinusoidal voltages.

The system represents the implementation of the horizontal-sweep method, which is based on the Cauchy-Riemann conditions for analytic functions. It provides a comparatively fast repetitive output of the phase information and hence makes the complex-plane scanner capable of being used for solving the approximation problem of network synthesis, when both the amplitude response and the phase response are specified.

PREFACE

A special analog computer called the complex-plane scanner has been built at the Department of Electrical Engineering of the University of Manitoba, and was described by E.P. Valstyn in his M. Sc. Thesis (see bibliography). It used the perturbation method of Ragazzini and Reynolds for the computation of the phase of network functions. This method is inaccurate because it depends on the measurement of small increments. A second method due to Kranc, Mauzey and Wuorinen is very accurate, but was not used, because it requires as many separate direct-reading phasemeters as the maximum number of poles and zeros to be accommodated, and hence becomes very expensive.

In this thesis a third method, called the horizontal-sweep method, will be described and its implementation will be discussed. It is hoped that the system using this method will be considerably more accurate than the perturbation method and at the same time, less expensive than that employed by Kranc, Mausey and Wuorinen.

The system consists of an imput unit and an output unit, and it uses the same central unit as the amplitude system. The input unit has been constructed and it will be described in detail. Due to a lengthy illness of the author, the output unit could not be built, so only its projected design will be described. Also, the performance tests of the overall system can only be obtained when the output unit is operational.

This thesis consists of four chapters. Chapter I deals with the underlying theory, its application and the expected limitations of the horizontal-sweep method. Chapter II presents the outline of the overall system. In Chapter III the details of the circuits comprising the input unit are discussed and in Chapter IV the arrangement of the proposed output unit is set forth.

The author is deeply indebted to the National Research Council of Canada for their financial support of this project. He also wishes to thank Professor R. A. Johnson for his able supervision of the project and for his suggestions and advice. The help received from Mr. T. J. White and Mr. R. D. Woods is greatly appreciated.

TABLE OF CONTENTS

CHAPTER IV

The Proposed Output Unit

LIST OF FIGURES

LIST OF FIGURES - Continued

CHAPTER I

THEORY AND APPLICATIONS

1. The Complex-Frequency Plane

Any network function F(s) - input immittance[1], transfer immittance, or dimensionless transfer function - of a system consisting of lumped parameters only is a rational fraction in the complex frequency $s = \sigma + jw$, i.e., it is the ratio of two polynomials in s:

$$F(s) = \frac{a_n s^n + a_{n-1} s^{n-1} + \cdots + a_1 s + a_o}{b_m s^m + b_{m-1} s^{m-1} + \cdots + b_1 s + b_o} \qquad (1)$$

(Gu 1 pp 315-317, St. 1, Ch. 2)[2]. The two polynomials can be expressed as the products of their root factors so that:

$$F(s) = \frac{H(s-z_1)(s-z_2)\cdots(s-z_n)}{(s-p_1)(s-p_2)\cdots(s-p_m)} \qquad (2)$$

where $H = \frac{a_n}{b_m}$, positive real constant.

The z's and p's are the so called critical frequencies of F(s). $z_1, z_2 \cdots z_n$ are called the zeros, and $p_1, p_2 \cdots p_m$ are called the poles of the network functions.

---

1. Immittance is a generic word, introduced by H.W. Bode for both impedance and admittance. (Bk. 1, p. 15).

2. The abbreviations in parentheses refer to the bibliography.

From equation (2) it is clear that, except for the constant multiplier, the function F(s) is completely defined by its poles and zeros, which, since they are roots of the polynomials are either real or, if complex, must occur in complex-conjugate pairs.

The poles and zeros of a network function can be plotted in the complex-frequency plane or s-plane (see Fig. 1) and this, except for the constant multiplier H, is a complete graphical representation of the function. The excitation frequency s is

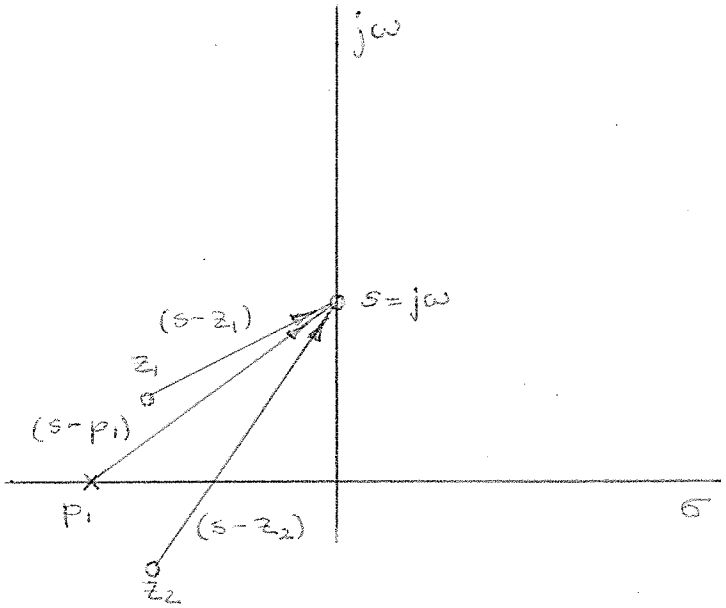

Fig. 1. Frequency factors.

a simple variable point that can be moved to any location in the plane. If only sinusoidal excitations are considered, the point s is constrained to the jw - axis.

A root factor $(s - z_k)$ - in circuit theory often called a frequency factor - appears in the s-plane as a phasor from the fixed point z_k to the variable point s, as shown in Fig. 1. Hence the magnitude and phase angle of a network function can be determined graphically from the s-plane plot of its poles and zeros. The magnitude is found by measuring the magnitudes of the frequency phasors, multiplying H by the magnitude of all those frequency phasors pertaining to zeros and dividing by the magnitudes of the phasors belonging to poles, since,

$$|F(s)| = H \frac{|s - z_1|\,|s - z_2| \ldots |s - z_n|}{|s - p_1|\,|s - p_2| \ldots |s - p_m|} \qquad (3)$$

For the determination of the phase of F(s) the phase angles of all the frequency phasors have to be measured. The phase of F(s) is then found by adding the phase angles of those phasors pertaining to zeros and subtracting from this sum the phase angles of the phasors belonging to poles, which corresponds to the equation:

$$\text{Arg } F(s) = \sum_i \text{Arg } (s - z_i) - \sum_j \text{Arg } (s - p_j) \qquad (4)$$

2. The Principle of the Complex-Plane Scanner

In the complex-plane scanner, sinusoidal voltages can be generated such that each of them corresponds to a frequency factor, $(s - z_i)$ or $(s - p_j)$, in equation (2), i.e., the phase of such a sinusoidal voltage is equal to the phase angle of the corresponding factor and its amplitude is proportional to the magnitude of the factor. This is achieved by

generating a proportional sinusoidal voltage for each pole and zero, and adding its negative to a sinusoidal voltage corresponding to s. This is illustrated in Fig. 2, where the voltages (or complex numbers) are represented

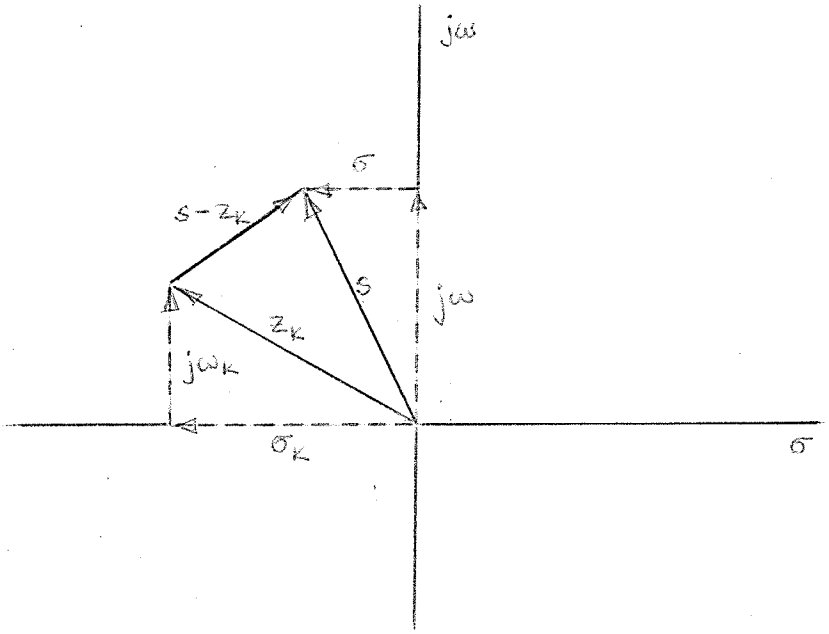

Fig. 2. Generation of Voltages Representing Frequency Factors.

by phasors in the conventional way. The voltages representing Z_k and s are generated in their turn by adding voltages corresponding to their real and quadrature parts, as shown in Fig. 2.

($z_k = \sigma_k \neq jw_k$ and $s = \sigma \neq jw$).

With the aid of logarithmic attenuators and peak detectors, the complex - plane scanner converts each sinusoidal voltage corresponding to a zero factor, $(s - z_i)$ into a d-c voltage, $A \ln | s - z_i | \neq B_i$, and

each sinusoidal voltage corresponding to a pole factor, $(s - p_j)$ into a d-c voltage $-(A \ln |s - pj| + Bj)$. These voltages are then added by a summing amplifier and, if A is made a constant of the computer, the resulting voltage is

$$V(s) = A\left(\sum_i \ln |s - z_i| - \sum_j \ln |s - pj|\right) + C$$

where $C = \sum_i B_i - \sum_j B_j$

The additive constant B_k - and hence the constant C - are introduced by the logarithmic attenuators and peak detectors, but are of no consequence, since they merely cause a constant drift in the voltage level.

Now, from equation (3),

$$\ln |F(s)| = \sum_i \ln |s - z_i| - \sum_j \ln |s - pj| + \ln H$$

so that the output voltage

$$V(s) = A \ln |F(s)| + D$$

where $D = C = \ln H$, or

$$\ln F(s) = KV(s) + E$$

where $K = \frac{1}{A}$ and $E = \ln H - KC$. This means that the output voltage of the complex-plane scanner varies with s as the logarithm of the gain function times the known constant A. If in Fig. 2, σ is made to vanish so that $s = jw$, then the output voltage

$$V(jw) = A \ln |F(jw)| + D$$

and if the jw - axis is scanned, i.e. if the voltage representing w is is made to increase uniformly with time, then a display of the output voltage vs. time (by oscilloscope or pen recorder) will give the frequency response.

3. The Horizontal - Sweep Method.

Computation of the logarithm of the gain function makes it possible to compute the phase slope or delay, and the phase of a network function without actually measuring the phase angle of each phasor representing a root factor and then forming their sum. This latter method has the disadvantage that it requires a separate phasemeter for each pole and each zero.

The horizontal-sweep method uses the fact that the real and imaginary parts of a function of a complex variable are not independent, but one can be computed from the other. If the logarithm of the function is taken then this statement applies to the magnitude and angle of the function.

From complex-variable theory

$$\ln F(s) = \ln |F(s)| \angle\ j \operatorname{Arg} F(s)$$

and at all points at which $\ln F(s)$ is analytic, i.e., everywhere except at the poles and zeros, the Cauchy - Riemann conditions (Ch. 1, pp 28, 29) give

$$\frac{\partial \ln |F(s)|}{\partial \sigma} = \frac{\partial \operatorname{Arg} F(s)}{\partial w}$$

If ω is kept constant at ωa and σ is varied linearly with time from $-\sigma a$ to $+\sigma a$ as shown in Fig. 3(a), i.e. if the

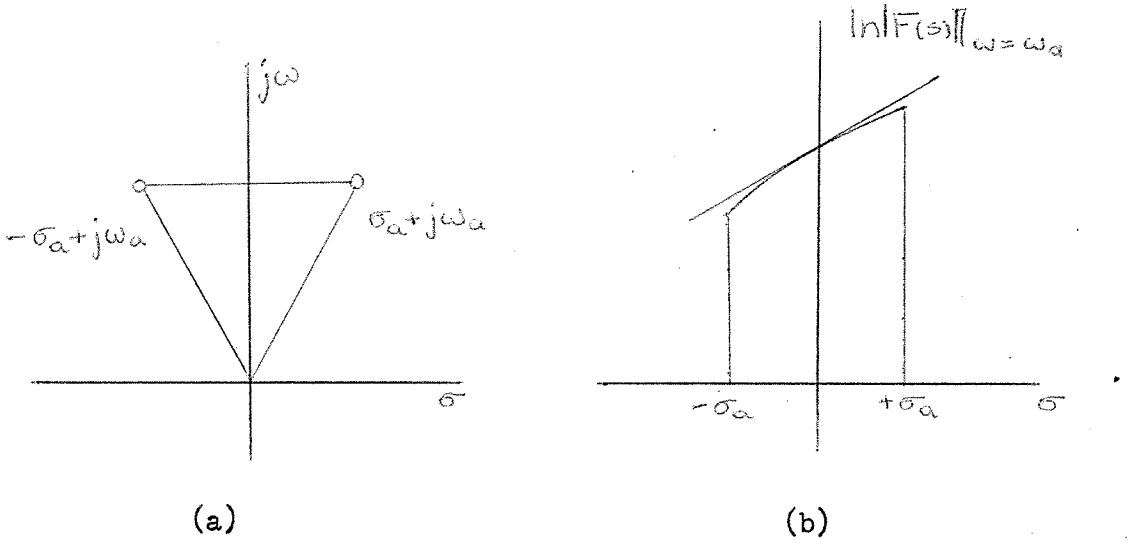

(a) (b)

Fig. 3. Illustration of the Horizontal-Sweep Method

scanning is done in the horizontal direction, then the output voltage of the computer will represent the function

$$\left(\ln |F(s)|\right)_{\omega = \omega_a}$$

Since only σ is varied, the slope of the function is

$$\left.\frac{d \ln |F(s)|}{d\sigma}\right|_{\omega = \omega_a} = \left.\frac{d \text{ Arg } F(s)}{d\omega}\right|_{\omega = \omega_a}$$

and the slope at the point $\sigma = o$ (see Fig. 3b).

$$\left.\frac{d \text{ Arg } F(s)}{d\omega}\right|_{s = j\omega a}$$

But this is the phase slope of the steady-state response at the frequency ω a.

This shows that the phase-slope can be computed by differentiation of the logarithmic amplitude function with respect to σ. But since electronic differentiation is only possible with respect to time, σ has to be made a linear function of time, i.e., the amplitude of the sinusoidal voltage representing a σ has to increase uniformly with time. Then the derivative of $\ln |F(s)|$ with respect to time will be proportional to its derivative with respect to σ.

Since the independent variable s sweeps parallel to the σ- axis, or horizontal axis of the complex plane this method is called the horizontal sweep method.

It is apparent that the method cannot give a perfectly continuous curve of phase slope against frequency, but only samples of the phase slope at a selected number of points or values of ω. If the number of points is quite high, a very smooth curve can be drawn through them so that the representation is quasi-continuous.

4. Automatic Horizontal Sweep.

To make the computation of phase slope and phase automatic it is necessary to scan the $j\omega$- axis in discrete steps. Between steps ω is to remain constant for a certain time period in which σ varies continuously from some negative to some positive value, thus causing the point representing the independent variable s in the complex plane to move from

left to right across the $j\omega$- axis. During this time the amplitude circuits of the complex-plane scanner compute $\ln |F(s)|_{\omega = \omega_a}$. This function of σ has to be differentiated and sampled when $\sigma = o$. If there is a large number of steps of ω and if the speed of scanning is high, then the samples of phase slope will also be numberous and they will occur in rapid succession. A hold circuit and a smoothing filter can then convert these samples into a slowly varying voltage representing the phase slope, and this voltage can be integrated to give the phase.

5. Factors which Influence the Choice of the Operating Speeds, Number of Steps, Width of Sweep and Gate Duration.

It is necessary to give a brief outline of the operation of the complex-plane scanner with an explanation of the terms to be used in the following paragraphs.

In the complex-plane scanner the sinusoidal voltages, which are the analogs of the vectors in the complex plane defining the σ and ω axes, are called carrier signals. The scanning of the complex plane is done by amplitude - modulating these carrier signals and adding them. By using proper modulating signals, the independent variable can be made to traverse any desired trajectory in the complex plane. The function, $\ln |F(s)|$ is the modulation envelope of the output signal of the logarithmic attenuator units, and has to be recovered from the carrier, which is done in the peak detector.

In order to allow a higher repetition rate, the carrier frequency had to be increased from 400 cps to 1600 cps. This is particularly important for the phase computation, since a comparatively high repetition rate and a large number of samples require a fairly high σ-sweep frequency. For oscillographic display of the phase output the repetition rate was chosen as $\frac{1}{2}$ cps. This means that the frequency of the ω-sweep is $\frac{1}{2}$ cps, and if there are to be 100 steps or sampling points, then the σ-sweep frequency becomes 50 cps. This is about the highest sweep frequency possible, because the detector response to the modulation envelope falls off rapidly above 100 cps.

The discharge time constant of the peak detector represents a compromise between the carrier frequency and the highest modulation frequency. The time constant was set at 2 m sec which is 3 times the period of the carrier and about one fifth of the period of the highest expected modulation frequency of 100 cps. This still leaves a large amount of 1600 cps ripple and further filtering is required.

The ability of the detector to follow the modulating envelope, i.e. the function $\ln|F(s)|$ depends on the speed of variation of that function, which in turn depends on the sweep speed, the sweep width and of course, on the character of the function itself. The fastest variation of $\ln|F(s)|$ occurs for critical frequencies close to the $j\omega$-axis.

Consider the complex plane with a zero located very close to the $j\omega$- axis, (Fig. 4) and let the independent variable s sweep through this singularity parallel to the σ- axis for the full possible sweep

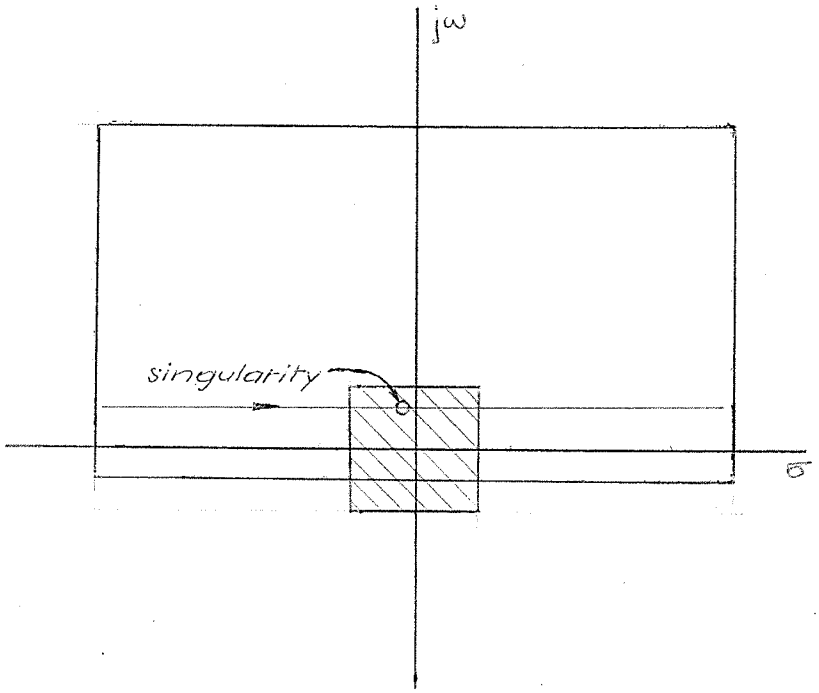

Fig. 4. The σ- sweep in the complex plane.

width of 10 units, i.e. five times the linear extent of the cross-hatched area to which the critical frequencies are confined.

As a result of this large sweep width the logaten input traverses its maximum range of three decades. The detector output is then approximately as shown in Fig. 5, i.e. a logarithmic curve. The sweep speed is assumed to be very slow so that the detector can follow the curve.

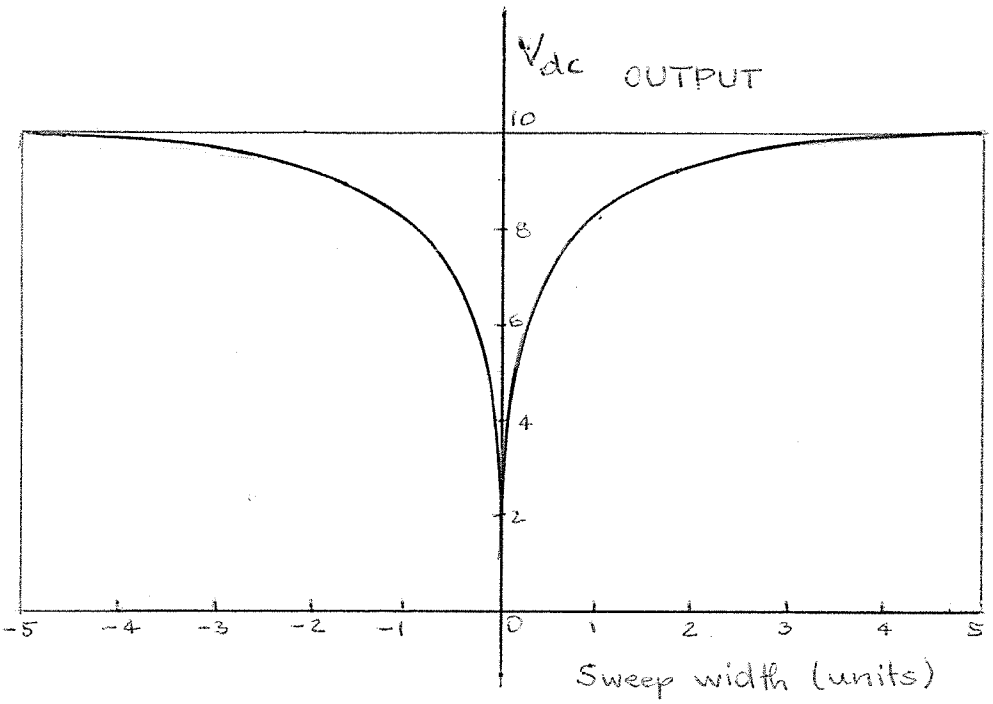

Fig. 5. Detector output at maximum sweep width.

Since the logarithmic curve encompasses three decades, the central dip where the zero is located is very sharp. The phase slope information is given by the slope of this curve at the point where it crosses the $j\omega$-axis. This shows that it is not necessary for the σ- sweep to traverse the full width of 10 units. A sweep-width of .2 units appears to be ample.

In Fig. 6, the detector output for the reduced sweep width is shown. It ranges over 1.3 decades of the logarithmic curve. The dotted line in the center, within $\pm$ .005 units, indicates the region where the logaten output is no longer proportional to the logarithm of the input.

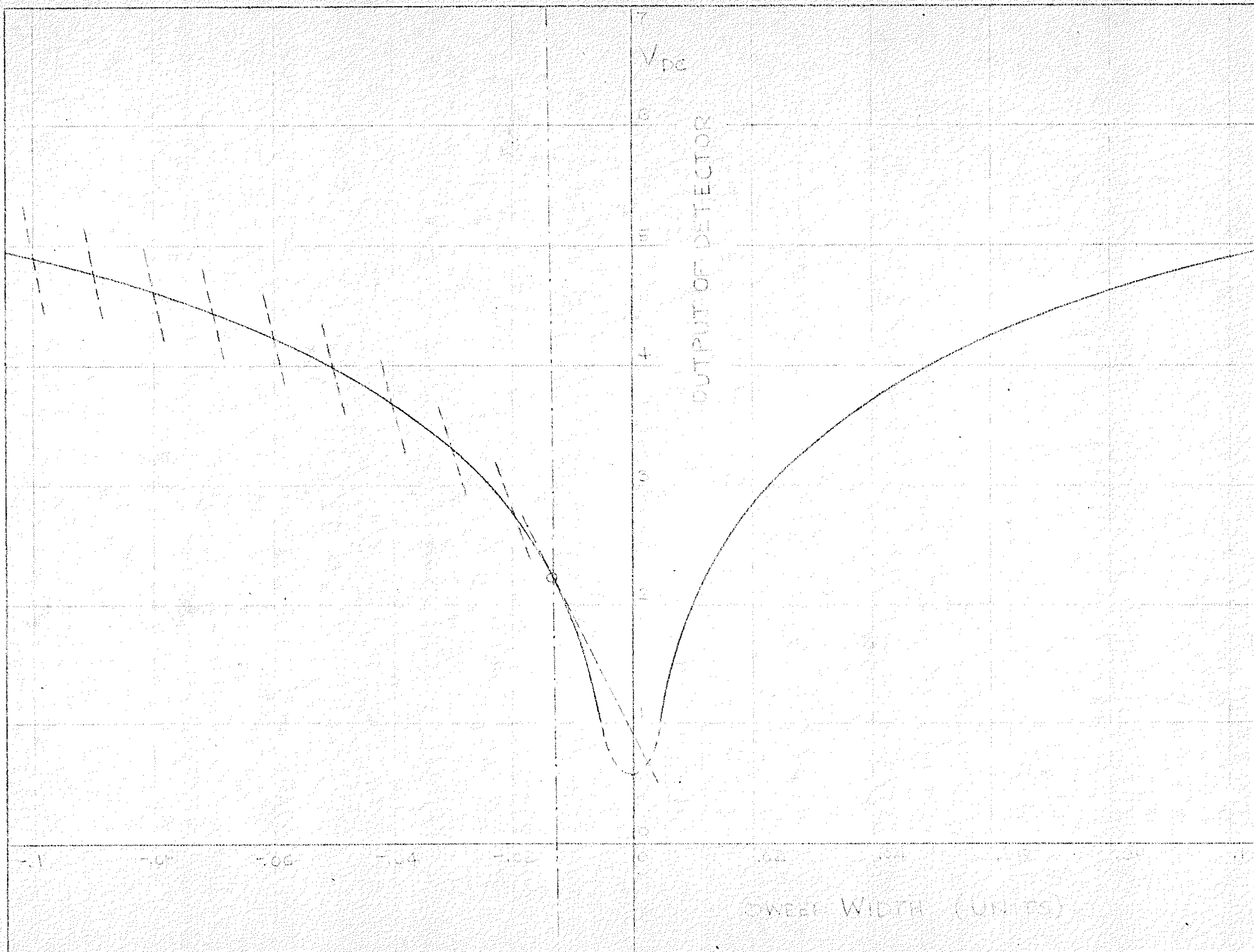

FIG. 5 DETECTOR OUTPUT AT REDUCED SWEEP WIDTH

In the diagram of Fig. 6, the sweep width is measured from the zero location. The $j\omega$-axis is shown as a dot-dashed vertical line. It can be seen that by decreasing the sweep width by a factor of 50 the sweep speed has also been reduced by a factor of 50, assuming that the time for one complete sweep is kept constant.

Since the frequency of the σ - sweep was chosen as 50 cps, then the period of the left-to-right sweep is 20 msec less the flyback time, which will be neglected here. Also the time constant of the detector was set at 2 msec. The initial slope of the discharge curve of a capacitor is such that, if it continued with the same slope, it would intercept the time axis at the value of the time constant. In Fig. 6 the maximum rate of fall of the detector output is indicated at different points on the curve by short dotted lines. These indicate that the detector cannot follow the curve beyond the point -.012 on the horizontal scale. This is based on the assumption that the detector response is limited only by its discharge time constant and not by any of the following filters. Hence .012 units is the minimum distance from the $j\omega$-axis of any zero, for which the phase computation will be reasonably accurate.

A complex conjugate pair of poles or zeros whose distance from the $j\omega$-axis is .012 unit, or smaller, represents a highly underdamped system with a very highly peaked response, i.e., the system has a resonant frequency with a very high Q. For such systems the standard

procedure of mathematical analysis using the narrow band approximations yields good results without excessive labor, so that an automatic computing device is not needed in this case.

The minimum distance of a pole or zero from the $j\omega$-axis is also limited by the number of samples of the phase slope which are computed. If ω is swept over 5 units then the spacing of the sampling points is .05 units. Hence for critical points which are closer to the $j\omega$-axis than .05 units, the number of sampling points is too small, because the phase will be changing more than 45° between two of these points. This limitation could be overcome by attenuation of the ω-sweep voltage by a factor of 5, say, so that it sweeps only over one unit. This would yield a "magnified picture" of the region where most of the change in the function occurs. The gate duration has to be small, so that, the output of the gate may represent, as nearly as possible, the instantaneous value of the derivative of $\ln |F(s)|$, as the independent variable s passes through $\sigma = 0$.

A gate duration of 2 msec was chosen, which corresponds to .02 units in the complex plane. In Fig. 6 it can be seen that the slope of the detector output changes too rapidly during the open period of the gate, when the zero is closer to the $j\omega$-axis than .02 units. Hence the accuracy in the case of critical points which are very close to the $j\omega$-axis is also limited by the gate duration.

On the other hand the gate duration has to be at least as long as the period of the carrier, otherwise even a very small residual carrier ripple can cause large errors in the computed slope.

In Fig. 7, the amplitude of the ripple is much smaller than the rise in average level (dotted line), and still the variations in slope are extremely large. In order to provide a small factor of safety, let the gate duration be equal to three periods of the carrier, which is

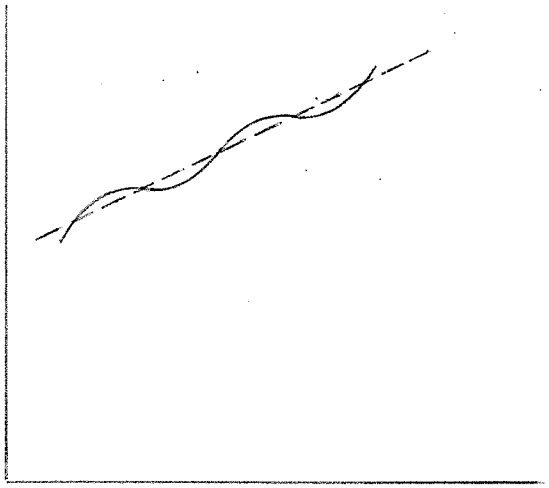

Fig. 7. Carrier Ripple Superimposed on the Output

2 msec. Let the function $\ln |F(s)|$ be given by

$$y = ax + b \sin 6\pi x$$

for a short period of time. In an interval of one unit in x, there are 3 cycles of the sine-wave of maximum amplitude b and the average level

rises by an amount a. The derivative of this function is

$$\frac{dy}{dx} = a + 6\pi b \cos 6\pi x$$

The maximum and minimum slopes of this function are $a + 6\pi b$, and $a - 6\pi b$ respectively. The slope will never become negative if $a > 6\pi b$. This means that the amplitude of the carrier ripple must be less than 5% of the rise in the average level which gives the true derivative of $\ln |F(s)|$. Hence extremely good carrier filtering is required, in order that small phase slopes may still be detectable. This filtering can be partially carried out after the differentiation.

The transfer function of a channel from logaten input to detector output is

$$V_o = 3.0 \log_{10} V1 + 7.9.$$

(the constants are approximate.) V1 is taken in units in the complex plane, and one unit corresponds to 1.2V rms in actual carrier voltage. Differentiating, we get

$$\frac{d V_o}{d V_1} = \frac{3.0}{2.303 V_1}$$

For $V_1 = 1$ unit i.e., for a critical point being 1 unit away from the $j\omega$-axis,

$$\left.\frac{d V_o}{d V_1}\right|_{V_1 = 1} = 1.305 \text{ volts/unit}$$

Since the gate duration covers .02 units, the constant a defined above becomes approximately 25 mV. Hence the carrier ripple should be less than 1 mV rms. Since the ripple in the output of each detector is about 70 mV rms, the total ripple voltage, when all twelve channels

are on, may reach about one volt at the worst. Therefore a very sharp low-pass filter is required, which must have a cut-off slope of 60 db per decade, and a passband of 160 cps.

The range of phase slopes of different functions to be handled by the complex-plane scanner may be 100 to 1 or greater. Clearly some range switching is required, in order to get good accuracy at both the low and the high ends of the range. For functions which have no critical frequencies close to the $j\omega$-axis, and therefore have small phase-slopes, it appears advantageous to increase the sweep width. This will increase the output signal in proportions to the increase in sweep width and hence will allow better discrimination against noise and carrier ripple.

CHAPTER II

OUTLINE OF THE SYSTEM

The system consists of an input unit, a central unit and an output unit. The input unit generates the sweep voltage which represents the independent variable s. The central unit, which consists of twelve channels establishes the analog of the critical frequencies and computes $\ln |F(s)|$, the logarithmic amplitude function. The output unit operates on the function $\ln|F(s)|$ so as to extract the phase information.

1. The Input Unit

The block diagram of Fig. 8 shows the overall interconnection of the circuits which generate the sweep voltage. The upper chain of blocks generates the σ - sweep and the lower one generates the ω - sweep.

It is desirable that the frequency of the σ - sweep be an exact submultiple of the carrier frequency. Therefore, a multivibrator frequency divider is used to divide the carrier frequency first by 16, and in another stage by two. The second multivibrator has an unsymmetrical waveform and is used for gating a sawtooth generator. The signal from the sawtooth generator is fed into a predistorter which distorts the sawtooth in such a way that, despite the non-linearity of the modulator, the modulation envelope is quite linear. The balanced modulator suppresses the modulating frequency and passes only the modulated carrier. The degree of modulation is about 50%.

A higher modulation percentage cannot be obtained without a serious drop in the linearity of modulation and distortion of the carrier.

In order to let σ vary from some negative to some positive value, a constant sinusoid, whose amplitude is equal to the average of the amplitude of the modulated wave and which is 180 degrees out of phase with the carrier of the modulated wave, is then added to the output of the modulator.

The staircase function is generated by integration of a series of spikes. These spikes are obtained from the multivibrator driving the sawtooth generator, by inversion, differentiation, and negative clipping.

The comparator is a monostable multivibrator which is biased so that it will be triggered when the output of the integrator has reached a certain value. The relay coil acts as the plate load of one of the two multivibrator triodes, so that the relay closes or opens when the multivibrator changes its states.

The contacts of the relay are used to set the integrator back to its initial condition. The initial condition voltage is obtained from an initial condition power supply, and it determines the point below the origin of the complex plane where the ω-sweep will start.

The output of the staircase generator is fed into the x-input of a Philbrick type MU/DV electronic multiplier. The carrier at a phase angle of 90° to the reference is fed into the y-input of the multiplier after amplification by a factor of 2 in order to take advantage of the full input range of the multiplier.

The σ - sweep and the ω- sweep are fed into the input summing amplifier and the complete sweep voltage is supplied to each of the 12 channels of the complex-plane scanner.

2. Modifications of the Central Unit

The central unit was built earlier (see Va. 1) with the main objective of getting good accuracy in the calculation of the logarithmic gain function. This same central unit was used for the phase computation by the perturbation method and will be used for the phase determination by the horizontal-sweep method with slight modifications.

The frequency of the reference carrier generator has been increased from 400 cps to 1600 cps. Also the filters in the peak detectors have been changed to this new frequency. This higher frequency makes it possible to operate the complex-plane scanner at a higher repetition rate.

3. The Output Unit.

The output of the central unit represents the function $\ln|F(s)|$, but it still contains considerable carrier ripple. The first block of the output unit therefore is a filter which attenuates this ripple to a very low value. The signal is then passed through a differentiator and sampled by a gate. This gate is driven by a delay multivibrator which is synchronized with the start of the σ-sweep. The delay has to be adjusted so that the gate opens when the σ-sweep crosses the $j\omega$-axis.

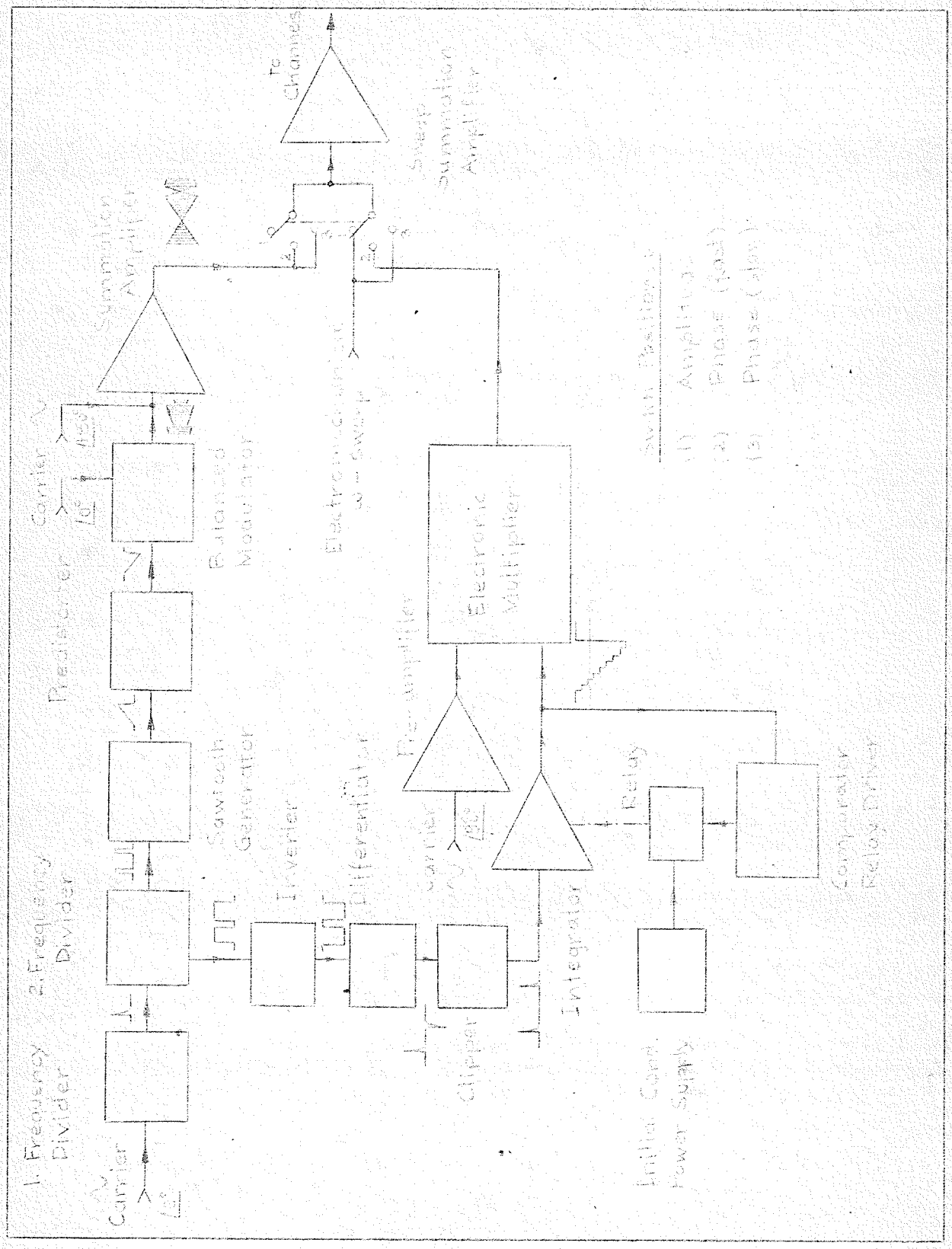

FIG. 5 BLOCK DIAGRAM OF INPUT UNIT

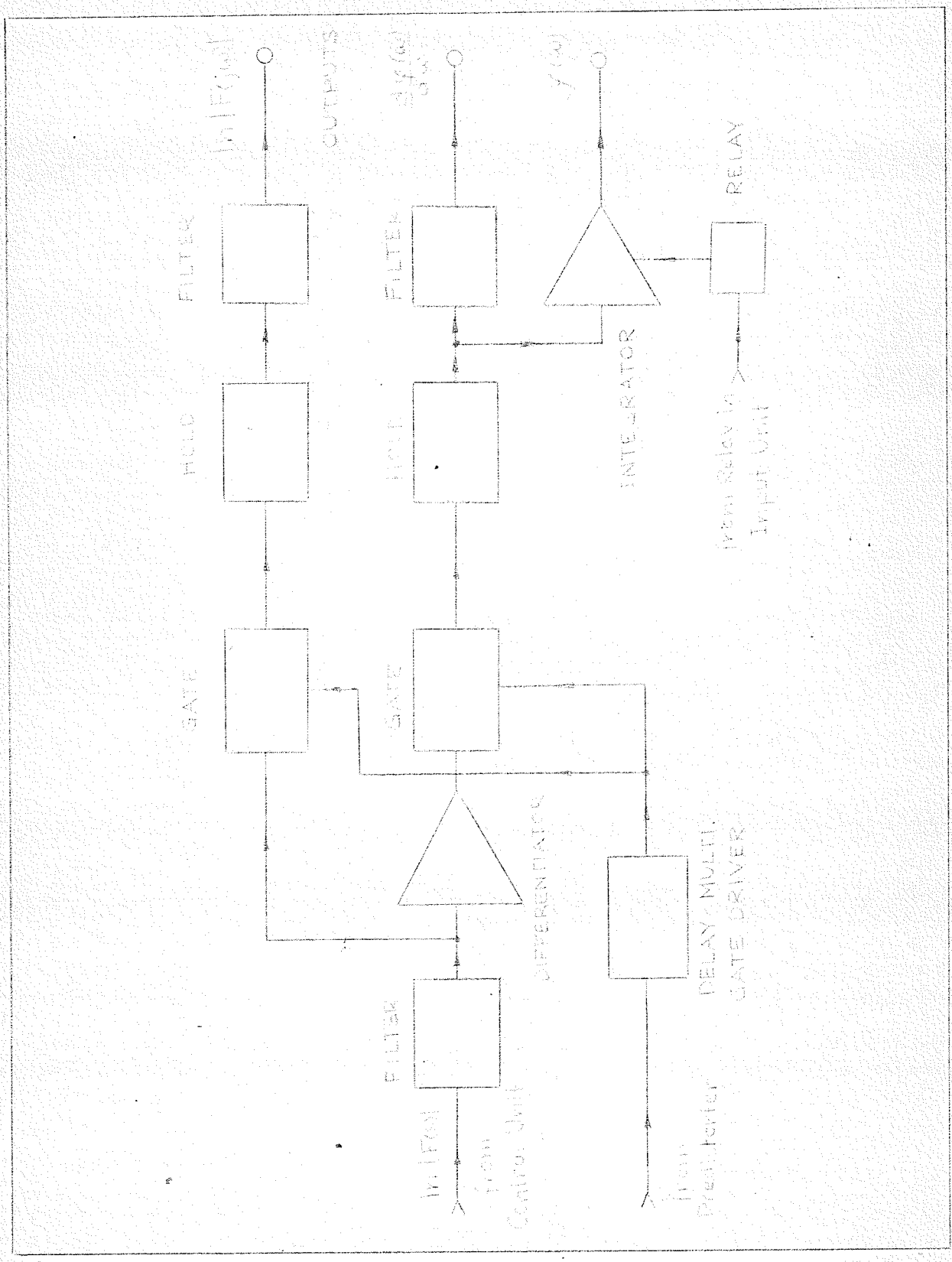

FIG. 6 BLOCK DIAGRAM OF OUTPUT UNIT

A sample transmitted by the gate is held by the hold circuit capacitor. This capacitor discharges extremely slowly while the gate is open, because the open gate has a back resistance of over 100 megohms and also the input resistance of the cathode follower, to which the hold capacitor is connected, is in excess of 100 megohms. When the gate is closed the hold capacitor quickly charges to the voltage appearing at the input of the gate, and this voltage can be positive or negative because the gate is bidirectional.

The output of the hold circuit is smoothed out to give a slowly varying voltage representing the phase slope. It is also fed through an integrator from which the phase as a function of frequency is obtained.

There is also a second chain of gate, hold and filter circuits, which operate directly on the $\ln |F(s)|$ signal and compute $\ln |F(j\omega)|$. Since the amplitude response is computed by the use of a continuous ω - sweep, without any σ - sweep this chain is not necessary and could be omitted.

CHAPTER III

THE COMPONENTS OF THE INPUT UNIT

1. THE FIRST FREQUENCY DIVIDER

A plate-coupled monostable multivibrator (Fig.11) is used to divide the frequency of the input sine-wave by 16. This is a fairly high division ratio and hence the stability of the divider becomes critical. Good stability is obtained by returning the grid leak resistors to the plate supply voltage. The input impedance at the grid of $T2_A$ for the 1600 cps carrier signal is about 50k, because there is a path through the .02μf capacitor and the 57k resistor of $T2_B$ to signal ground. This makes it necessary to use a .05 μf capacitor for coupling the carrier signal to the multivibrator with little attenuation. This is important because the stability of the divider is decreased, if the sine-wave signal superimposed on the discharge curve of the .02 μf capacitor is attenuated. But this large coupling capacitor also provides a low-impedance path for the multivibrator grid signal, and spikes would be fed back into the carrier signal source, if they were not isolated by the input cathode follower. The 25k potentiometer is used to vary the amplitude of the carrier input to the multivibrator, which has the effect of adjusting the division ratio. The spikes fed back from the multivibrator are superimposed on the carrier signal at the cathode of $T1_A$, so that this is a convenient test point, because the number of cycles of

the carrier between spikes can be counted on an oscilloscope and this number is the division ratio. Fig. 10 is an actual oscillogram of the waveform at the test point.

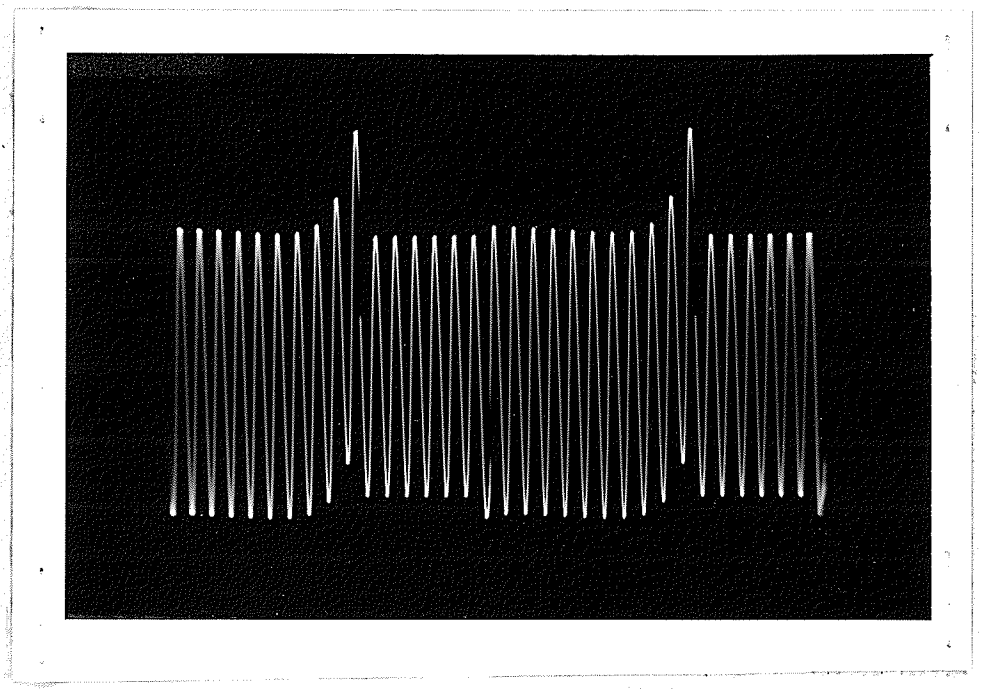

Fig. 10 Waveform at Test Point

The square wave from the plate of $T2_B$ of the multivibrator is differentiated by the 100 pf capacitor and the parallel combination of the 1M and 2.2M resistors, giving a time constant of 67 μsec and hence sharp spikes. These spikes are fed into a paraphase amplifier which is used as an isolating stage, so that the load on the multivibrator is very small and cannot affect its stability.

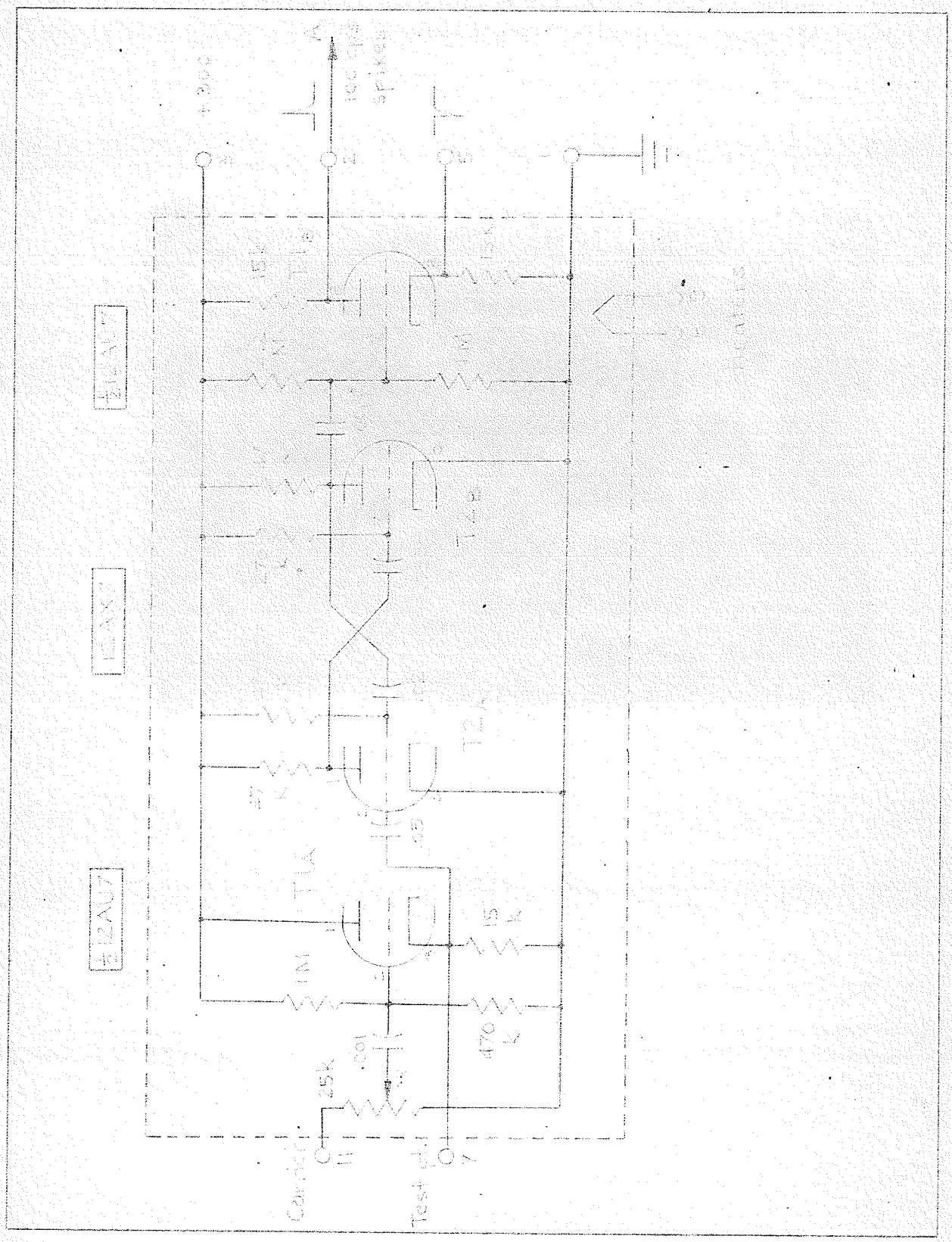
Ground
Test +

Also the paraphase amplifier provides both positive and negative spikes, so that either positive or negative triggering of the following multivibrator could be used.

Since the falling edge of the square wave is much steeper than the rising edge, it produces a much sharper spike or larger amplitude than the rising edge. This causes the signal at the grid of $T1_B$ to appear as if the positive spikes had been clipped.

The circuit diagram of the frequency divider is shown in Fig. 11. It is mounted in a Vector (type C12 NNK) can and the numbers of the external terminals correspond to those on the 11-pin plug on the Vector can.

2. THE SECOND FREQUENCY DIVIDER

A further frequency division by a factor of 2 is achieved by another multivibrator (see Fig. 12). Stability is not as critical as in the first frequency divider, and only one grid resistor has been returned to about $\neq$ 100 volts, which can be varied to adjust the free-running or natural period of the multivibrator. The multivibrator waveform was made asymmetric, with a ratio of the two periods of about 5 to 1, because it is used to gate the sawtooth generator.

The positive spikes from the first frequency divider are

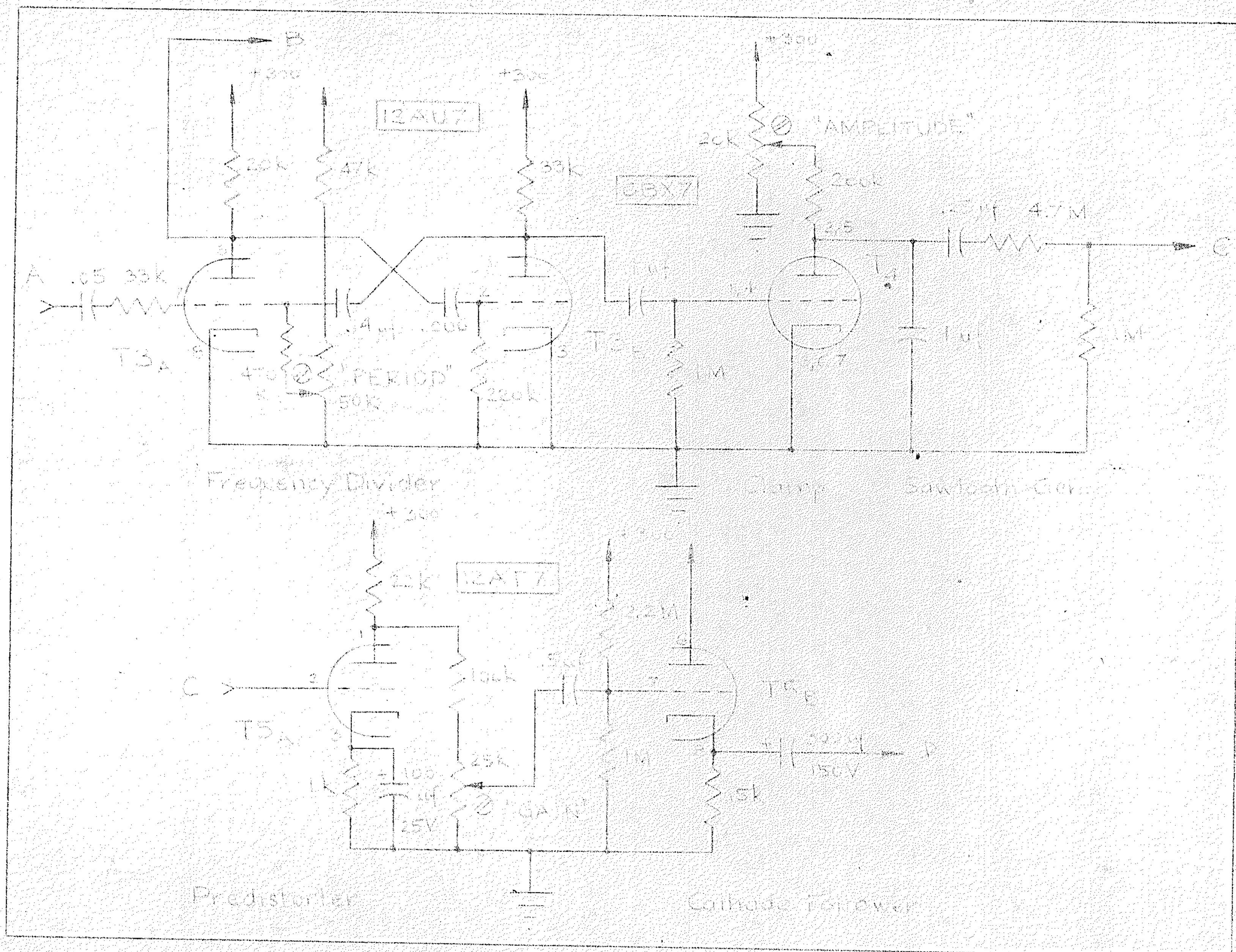

FIG. 12 2. FREQUENCY DIVIDER, SAWTOOTH GEN, PREDISTORTER AND CATHODE FOLLOWER

coupled to the grid of $T3_A$ through a .05 μf capacitor and a 33k resistor. This resistor was selected so that it does not attenuate the spikes too much, while at the same time it prevents the low output impedance of the paraphase amplifier from heavily loading the multivibrator.

3. THE SAWTOOTH GENERATOR

The top of the signal at the plate of $T3_B$ is clamped to ground level by the grid current flow from the 6Bx7 (see Fig.12). Because of the asymmetry of the square wave, the grid of T_4 is slightly positive for about 3 msec and cut off for about 17 msec. While T_4 is cut off, the 1 μf capacitor charges through the 200k resistor. Since the charging time constant is 200 msec. while the actual charging time is only 17 msec, the linearity of the rise is good. The sweep speed error is 8%, but this is not serious, because it will be compensated in the predistorter. A photograph of the sawtooth as it appears at the output of the sawtooth generator has been taken and is shown in Fig. 13.

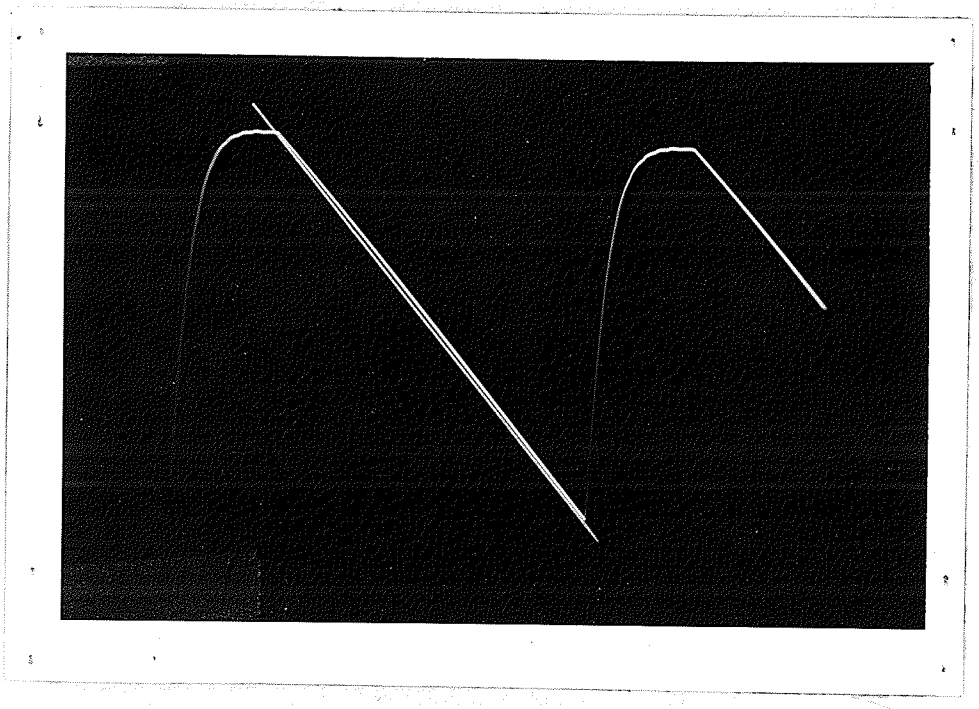

Fig. 13 Output of Sawtooth Generator

The curvature of the sawtooth is made apparent by the white straight line drawn on the photograph.

The discharge time constant is very short, because the high perveance 6Bx7, with the two triode sections in parallel, has a beam resistance of about 650 ohms. The amplitude of the sawtooth can be set by adjusting the 20k potentiometer, which changes the final voltage to which the 1 μf capacitor would charge up, if T_4 were continuously cut off. The maximum amplitude of the sawtooth across the capacitor is 25.5 volts peak to peak and its amplitude at the output C is then about 5 volts peak-to-peak.

Capacitive coupling to the next stage is used, because the amplitude adjustment changes the d-c level of the sawtooth output, and it is desirable to operate the next stage at constant bias. The reactance of the .25 μf coupling capacitor at 50 cps, which is the frequency of the fundamental component of the sawtooth wave, is about 13k, which is very much lower than the 5.7 megohm total resistance in series with it, and hence its effect on the waveform is negligible. The loading effect of the 5.7 megohm total resistance connected across the 1 μf capacitor is such that it reduces both the amplitude and effective time constant of the generated sawtooth by only 3.3%.

Originally the sawtooth generator was operated with a 1 sec charging time constant using a 1 M resistor and a 1 μf capacitor. This gave extremely good linearity of the sawtooth but also a small signal amplitude. In order to keep the sawtooth linear the grid leak resistor of $T5_A$ had to be as high as 10 MΩ. Due to this high impedance level and to the small signal amplitude the sawtooth generator was very susceptible to pickup. The voltage picked up had a frequency of 10 cps, which was probably a beat between the 50 cps sawtooth and the 60 cps line voltage.

Since the modulator following the sawtooth generator does not have very good linearity, predistortion of the sawtooth has

to be used to compensate for the distortion introduced by the modulator. Hence it is not very important that the sawtooth generator produce an extremely linear rise, because the deviation from linearity introduced by the sawtooth generator can also be compensated in the predistorter.

Using a time constant of .2 sec allows the sawtooth generator to operate at a higher signal level and also permits the coupling circuit to have a lower impedance level. As a result of these changes the pickup was reduced considerably. It was found that the sawtooth generator produces a negative-going wave. When its peak-to-peak amplitude was adjusted to 4 Volts then its positive peak was 2.5 Volts and the negative peak was -1.5 Volts. This could only be explained as a result of the Edison effect. An equivalent generator of voltage E_E with internal resistance r was assumed and the calculated waveform was related to the measured one. The values of E_E and r were found to be about -1.5 Volts and 500 ohms respectively. The calculations required to obtain these figures are given in the Appendix.

4. THE PREDISTORTER AND CATHODE FOLLOWER

The predistorter is simply an amplifier stage which is biased so that the input signal, which has a fairly large amplitude, drives the tube into a region where the distortion is relatively

high. The dynamic transfer characteristic of a triode and the plate current waveform resulting from a perfect input sawtooth is shown in Fig. 14.

The distortion produced is opposite to that produced in the sawtooth generator and in the modulator. The amount of predistortion depends on the input signal amplitude and on the bias, but the bias

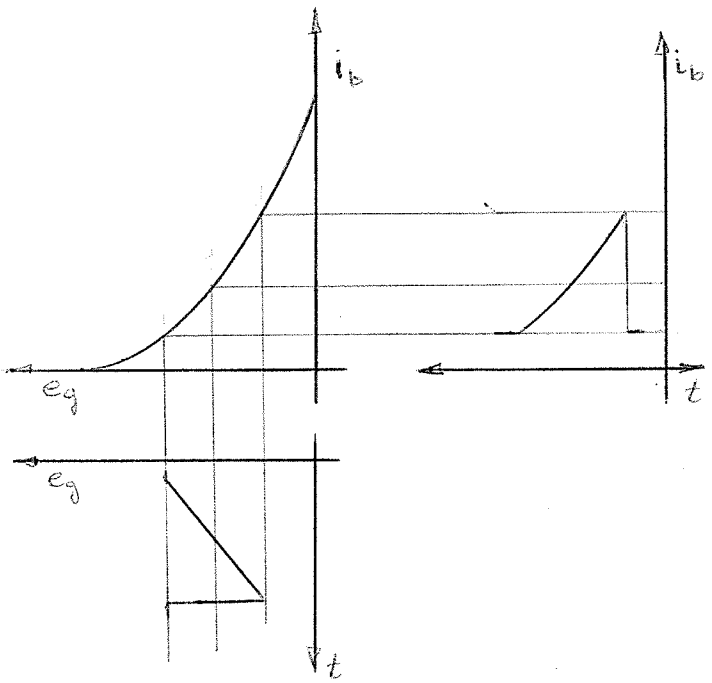

Fig. 14. Illustration of Predistortion

is fixed at a point where the predistortion is sufficient with a reasonable input signal. The amplified and inverted sawtooth appearing at the plate of $T5_A$ is attenuated so that its amplitude is correct for feeding the modulator. The two controls called "AMPLITUDE" and "GAIN", shown in Fig. 12, can be adjusted

simultaneously, such that the amplitude of the sawtooth signal fed to the modulator remains constant, while the amount of distortion changes.

The actual sawtooth output of the predistorter has been photographed and is shown in Fig. 15. A slight curvature opposite to that of Fig. 13 is noticeable.

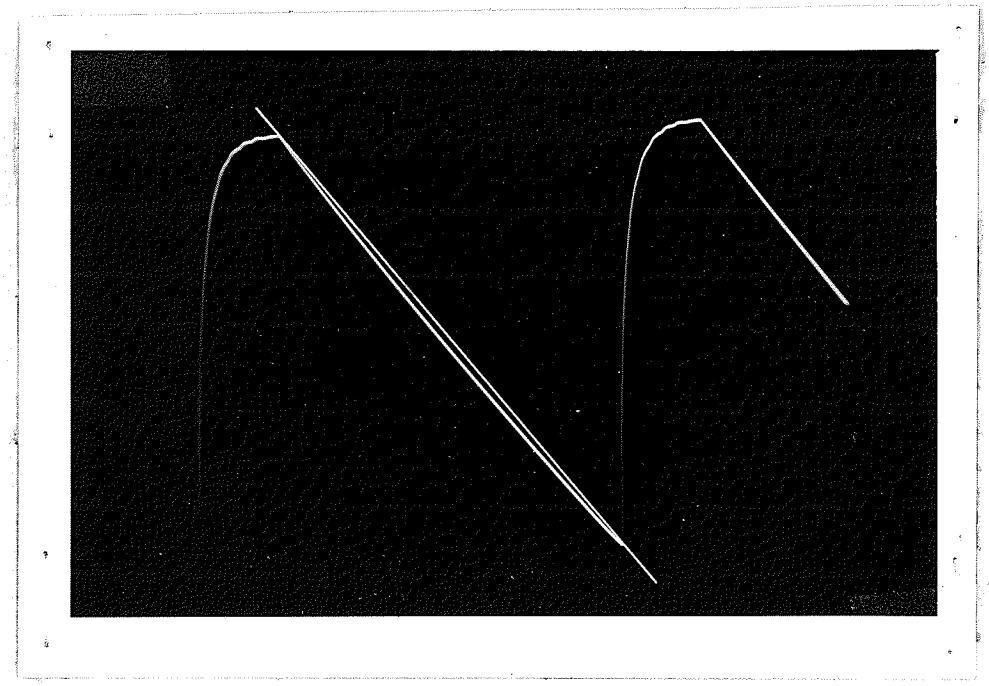

Fig. 15. Output of Predistorter

The cathode follower is used to obtain a low output impedance for driving the modulator. The low output impedance insures gain stability and hence a constant percentage of modulation.

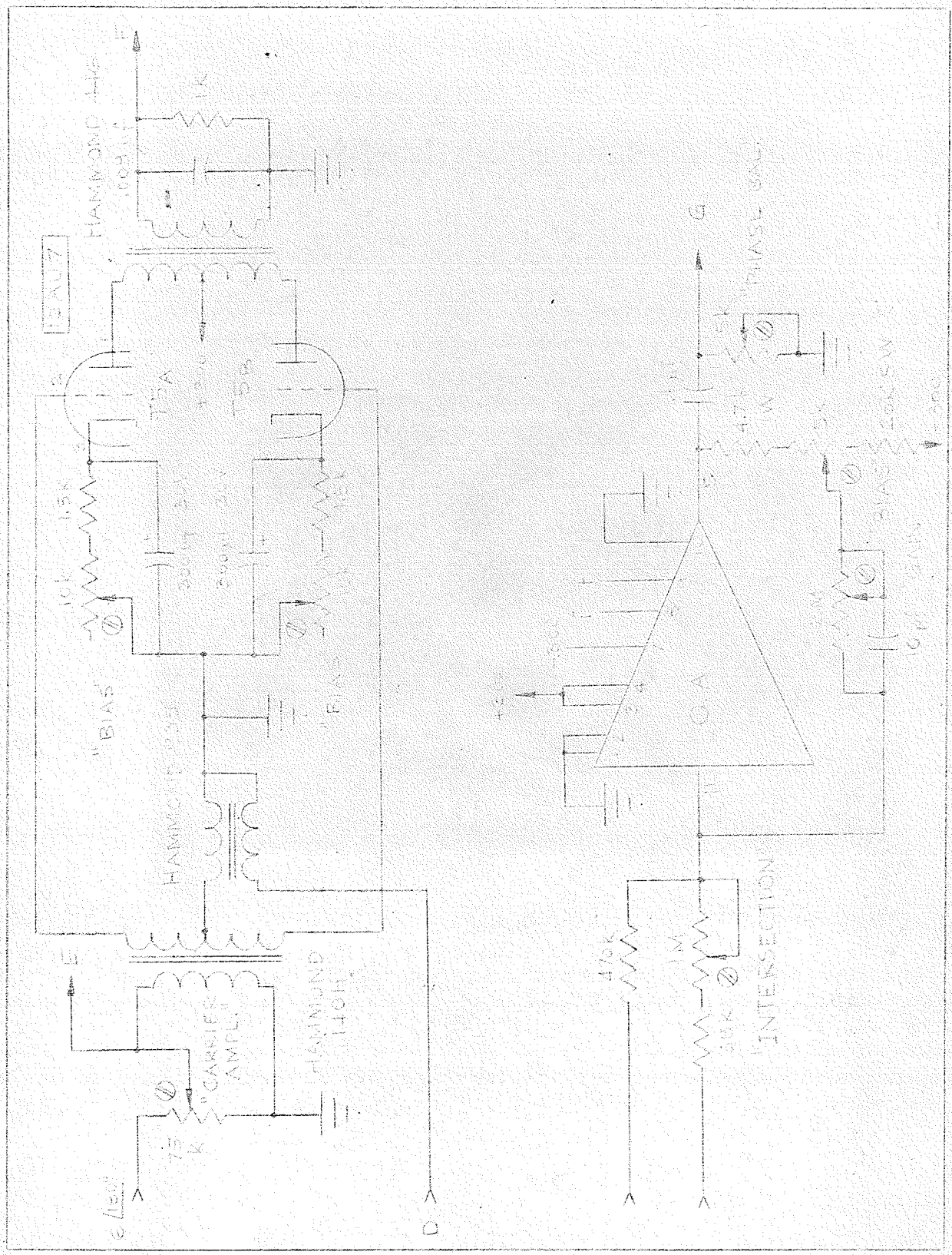

FIG. 8 ENHANCED MODULATOR AND ANTENNA

5. THE BALANCED MODULATOR

The carrier signal is fed to the grids of the modulator tubes in push-pull, while the modulating signal is fed in phase (see Fig.16). This results in the cancellation of the modulating signal components in the plate circuit of the modulator. The operation of the modulator depends on the fact that the transfer characteristic of a triode over a limited range approaches a parabola. Since the slope of a parabola is proportional to the abscissa, the transconductance of a triode, whose transfer characteristic is a parabola, is proportional to the grid potential. The relatively slowly varying modulating signal sets the bias about which the carrier oscillates, and hence the gain of the modulator, as far as the carrier is concerned, is proportional to the instantaneous value of the modulating signal.

A photograph of the modulated signal as it appears at the output of the modulator is shown in Fig. 17.

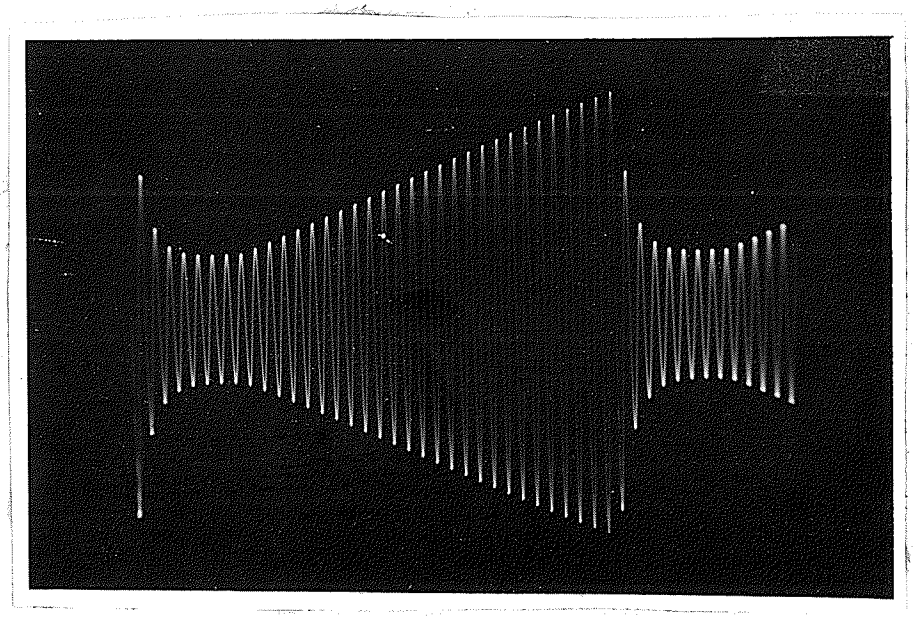

Fig. 17 The Output of the Modulator

Due to deviations from the square-law transfer characteristic, distortion of both the carrier waveform and the modulation envelope is produced. The bias of each modulator tube can be adjusted individually to select the region of most linear operation and to get exact balance ie. complete cancellation of the modulating signal component in the output. By means of the 75k potentiometer at the carrier input the amplitude of the carrier signal is adjusted to the highest value obtainable with negligible third harmonic distortion. Like any push-pull circuit the balanced modulator eliminates the second harmonic component.

Some phase-shift, (other than 180°), of the carrier signal occurs in the transformers and this is compensated by selecting the capacitor across the secondary of the modulator output transformer. The optimum value of this capacitor is that which gives the best null, as observed at the output of the adder.

6. THE ADDER

A feedback network is added to an operational amplifier so that an adder is obtained. The operational amplifier is of the same type as that used in the central unit of the complex-plane scanner (Va 1). The bias and gain controls are nearly independent.

The connections to the secondary of the modulator output

transformer are made such that the total phase shift through the modulator is 180°. Hence addition of the carrier signal, at 180° phase, to the modulator output, at 0° phase, amounts to a subtraction. A null will result where the two signals are equal in amplitude. The control called "Intersection" is used to vary the adder gain for the modulated signal only, until the null or intersection of the modulation envelopes occurs at the center of the sweep.

The purpose of the 10 pf capacitor across the 2 megohm feedback resistor is to reduce the high-frequency noise in the output of the adder. This and other capacitors inside the operational amplifier create some phase shift, which is compensated for by the "PHASE BALANCE" potentiometer in the output of the amplifier. This potentiometer together with the .1 μf coupling capacitor also forms a high-pass filter, which reduces the 10 cps ripple in the output. This ripple has the same cause as that described in the section on the sawtooth generator.

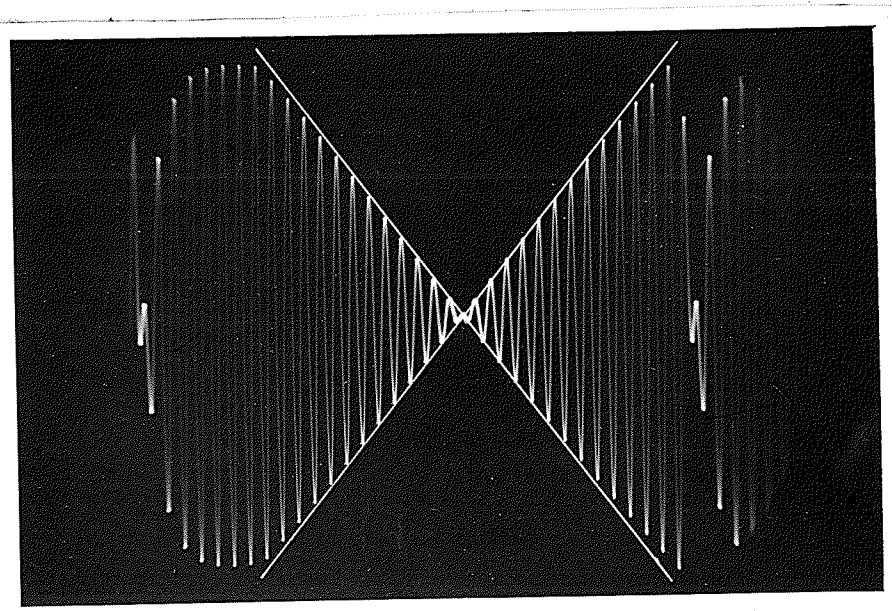

Fig. 18 σ-Sweep Voltage at Output of Adder

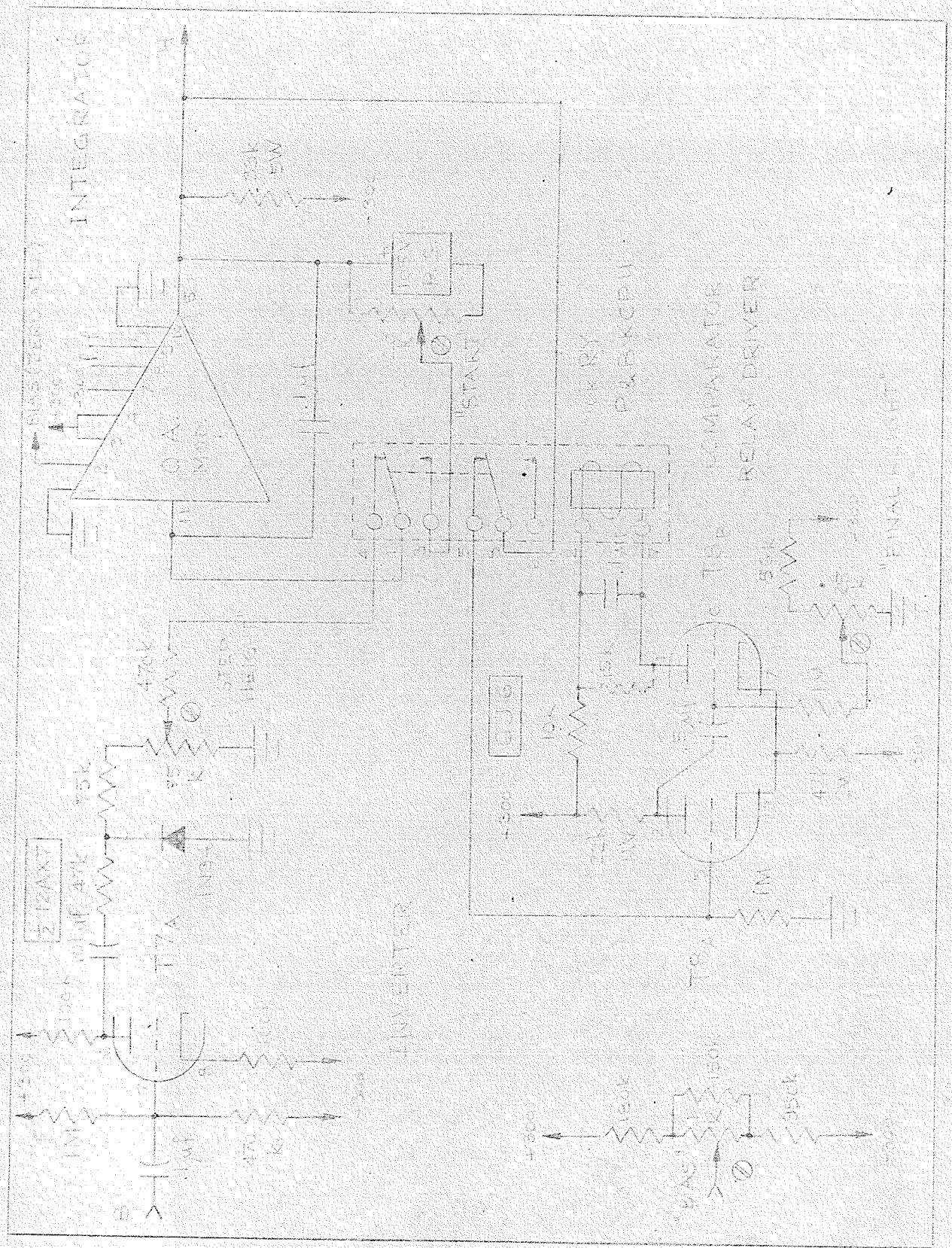

FIG. 19 TIMER AND FUNCTION GENERATOR

The final σ-sweep at the output of the adder is shown in the photograph of Fig. 18. The degree of linearity of the modulation can be judged by comparison with the straight white line drawn on the picture.

7. THE STAIRCASE FUNCTION GENERATOR

The square wave from the plate of $T3_A$ of the second frequency divider is inverted by $T7_A$ and differentiated to obtain spikes (see Fig. 19). The negative spikes are clipped by the IN34 diode. The positive spikes are integrated, resulting in a negative-going staircase signal. Since the time constant of the spikes is 2 msec, while their repetition rate is 50 cps, the staircase signal has steep "risers and flat "treads". The height of the steps can be adjusted by the 75k potentiometer at the input to the integrator. The integrator is made up of an operational amplifier of the type used throughout the complex-plane scanner. (Va 1) It was modified somewhat, because its basic design does not accommodate integration. The 180k resistor in the third divider chain was replaced by 470k, in order that the center of the $\pm$ 100 volt output swing may be near zero volts. The cathode of the first triode was not grounded, but was connected to a potentiometer in a bias chain. This allows the bias to be set such that, for zero volts on the grid, the output will stay at zero volts. Both modifications reduce the gain of the amplifier somewhat, but it is still adequate. Drift in the output for the 2 sec integrating time over a period of 15 min. amounts to about .3 volts which is small in comparison with

the output signal swing of 100 volts.

The RC time constant of the integrator is .05 sec and the gain of the amplifier after modifications is about 5000, hence the effective time constant of the integrator is 250 sec. The maximum integrating time for 1% accuracy is 2% of the effective time constant, i.e. 5 sec.

A DPDT Relay is used to set the initial condition of the integrator. It is driven directly by a comparator which serves to establish the output voltage at the end of the integrating time. In the position of the relay armature shown in Fig. 19 the spike input is connected to the integrator, while the initial condition power supply is disconnected. Also the output of the integrator is connected to the grid of $T8_A$ of the comparator. Triode $T8_B$ of the comparator is cut off by the negative bias applied to it and hence the relay stays open until the output of the integrator reaches a large enough negative value to trigger the comparator. $T8_A$ acts as a cathode follower, and since the two triodes have a common cathode, the bias of $T8_B$ is decreased until it reaches the cutoff value. The regenerative action of the monostable multivibrator circuit then causes the tube $T8_B$ to be clamped and $T8_A$ to be cut off. The current flowing through $T8_B$ energizes the relay and the armature is pulled in. Immediately both the connection of the integrator output to the comparator and the connection of the spike input to the integrator

are broken, and after a short time the input of the integrator is connected to the initial condition power supply. This power supply discharges the integrator capacitor and charges it to a smaller voltage of opposite polarity.

When the multivibrator is triggered $T8_A$ is cut off and the resulting rise in its plate potential is transmitted through the .5 μf capacitor, holding $T8_B$ in clamp. The .5 μf capacitor charges to the higher voltage through the 22k plate load resistor of $T8_A$ and the grid of $T8_B$ with a time constant of 10 msec. This causes the multivibrator to return to its stable condition, the relay armature is released and another cycle begins.

When the relay armature starts to pull in, it immediately disconnects the integrator output from the comparator. This is necessary because the sudden rise in the integrator output voltage when the initial condition supply is connected to the integrator capacitor, would immediately trigger the comparator, so as to cut $T8_B$ off and open the relay. This regenerative action is so fast, that the relay would not stay closed long enough to allow the integrator capacitor to charge fully to its initial voltage.

The initial condition power supply has a voltage of 105 volts, stabilized by an OB2 regulator tube. A 20 k potentiometer is connected across the supply which allows the initial condition voltage to be set. This voltage determines the point on the jω-axis

at which the ω-sweep starts, so the controlling potentiometer is labeled "Start".

The "Final Height" control sets the voltage at which the comparator will switch and hence determines the range over which the positive ω-axis is scanned. The "Step Height" potentiometer also has the effect of varying the integrating time, since the final height divided by the step height gives the number of steps during the integrating period, and the number of steps per second and the final height are held constant.

The circuit was arranged in the way described above, because it is most important that the range of ω-values be held stable, so that the ω-scale in the output will be dependable. The number of steps and the integrating time are of less importance. The resolution of the comparator is .1% and its stability .5%. The resolution is the change in input voltage required to pass from a reliable "off" condition to a reliable "on" condition (referred to the relay tube). The stability measures the shift in the required triggering voltage over a period of several minutes.

The waveform at the output of the staircase function generator is shown in Fig. 20. Because of their large number, the steps are so small that they are hardly visible. In fact the direct beam of the oscilloscope could not resolve them, and the photograph

has been obtained by making use of the persistence of the phosphor. Of course high contrast could not be achieved in this way because of the low intensity. The beam itself can be seen at the right of the picture as a very intense spot.

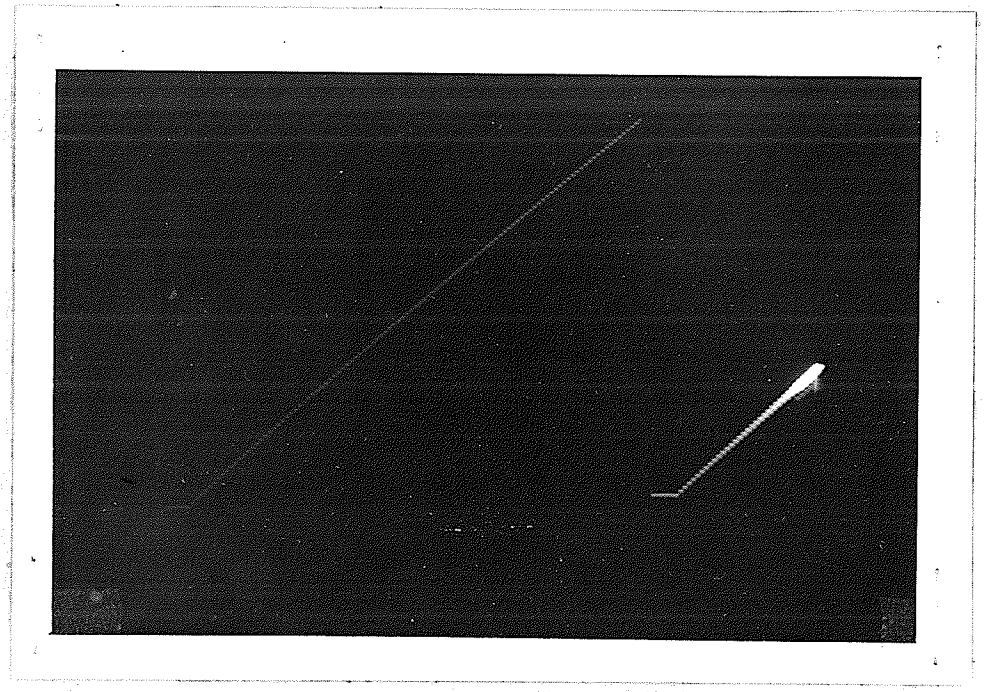

Fig. 20 The staircase wave

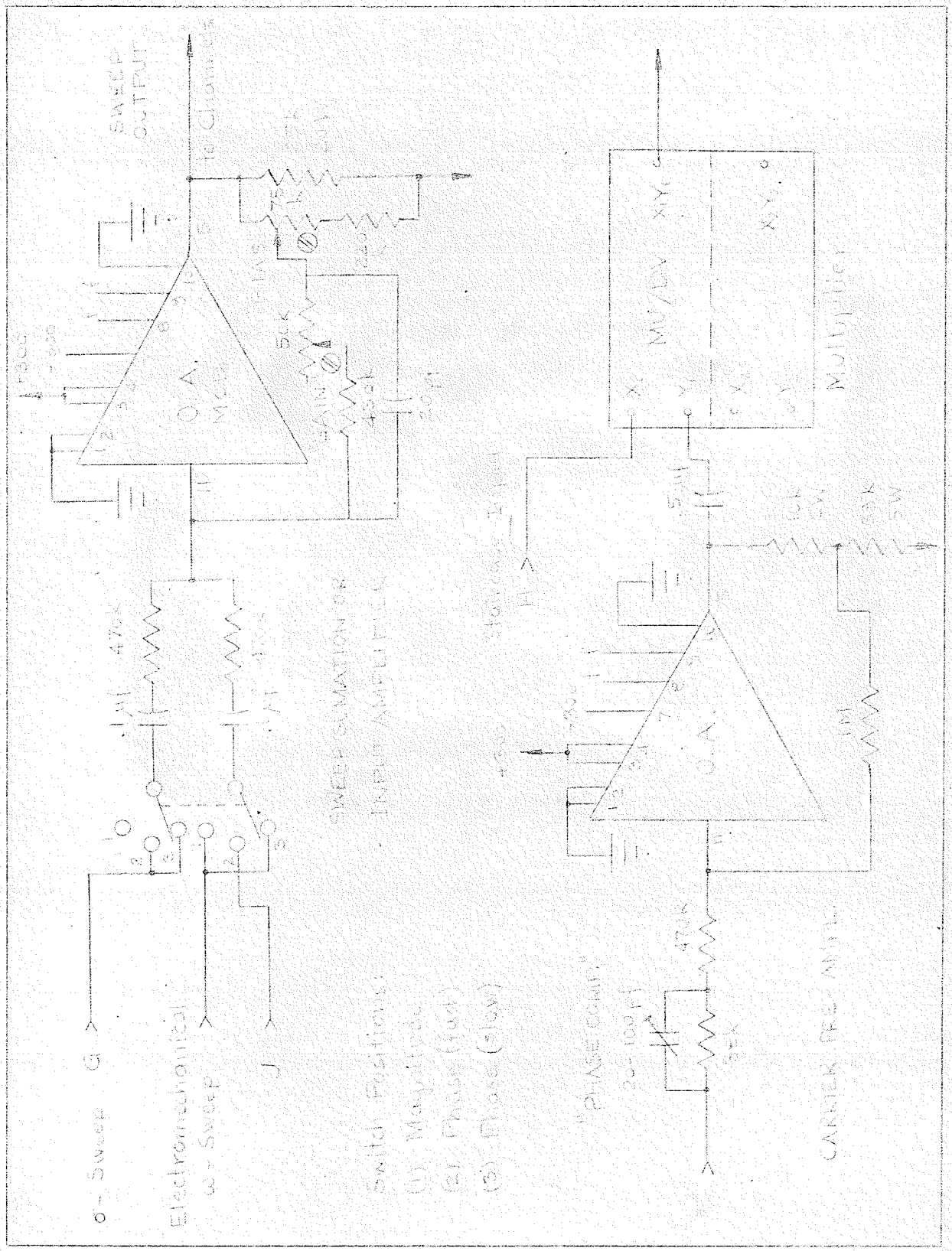

FIG. 20 CARRIER PROGRAMMED MULTIPLIER INPUT CIRCUIT

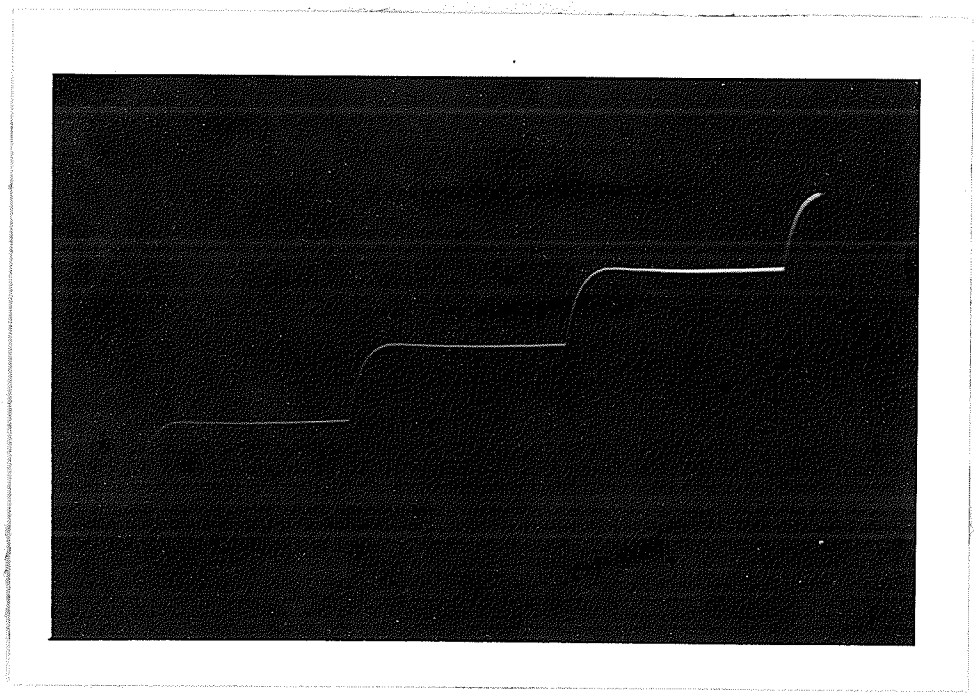

Fig. 21 Part of the staircase wave magnified.

Fig. 21 shows a part of the staircase signal magnified, so that one can study the detail of the steps.

8. THE CARRIER PREAMPLIFIER, THE MULTIPLIER AND THE INPUT AMPLIFIER

An operational amplifier of standard type (Va 1) is used to amplify the carrier signal by a factor of 2 before it is fed into the multiplier. This results in a multiplier input of about 35 volts peak-to-peak which is near its maximum input range of 50 volts peak to peak. The trimmer across the 39 k resister at

the pre-amplifier inputs is used to compensate for phase shifts introduced in the preamplifier, the multiplier and the sweep summation or input amplifier.

The multiplier is a Philbrick type MU/DV two-channel multiplier, but only one channel is used. The signal from the staircase function generator is fed into the X_1 input, and the amplified carrier into the Y_1 input. The output X_1 Y_1 ie. the carrier modulated by the staircase wave , is connected to the sweep summation amplifier.

A switch is arranged so that in position 1 only the slow w-sweep (generated by a motor-driven-potentiometer) is connected to the input amplifier, and the complex-plane scanner computes the magnitude of a network function. In positon 2 both the σ-sweep and the slow w-sweep are connected to the input amplifier and the complex-plane scanner computes the phase of a network function at a slow rate. Since in that position the complete w-sweep takes 15 sec, while σ sweeps at 50 cps there are 750 sampling points and it is not necessary to increase w in steps, because during one σ-sweep w increases only by a very small amount.

In position 3 the σ-sweep and the fast w-sweep from the multiplier are connected to the input amplifier. The speed of the

phase output is 2 seconds for the complete w-sweep and there are 100 samples. Since w changes appreciably between σ-sweeps the w sweep increases in steps, ie. it is staircase-modulated.

The function of the input amplifier is to sum the σ-sweep and the w-sweep. It has a low output impedance and ample current capacity to supply the sweep to all twelve channels.

CHAPTER IV

THE PROPOSED OUTPUT UNIT

1. THE FILTER

In order to get a cutoff slope of 60 db per decade, and at the same time a very flat curve inside the passband, a constant - k L-C filter was analysed.

A π - section requires only one inductance and its element values are given by the formulas (St. 1)

$$B = \frac{2}{\sqrt{LC}} \qquad (1) \qquad\qquad R_o = \sqrt{\frac{L}{C}} \qquad (2)$$

where B is the bandwidth in radians per second and R_o is the image impedance. L is the series inductance and C is the total shunt capacitance.

From formulas (1) and (2) the values of L and C become

$$L = \frac{2R_o}{B} \qquad (3) \qquad\qquad C = \frac{2}{BR_o} \qquad (4)$$

Since the bandwidth must be 160 cps or 1000 radians per second, and choosing R_o to be 1000 ohms, we get

$$L = 2h \qquad\qquad C = 2\,\mu f$$

The diagram of the constant -k π-section is shown in Fig. 23

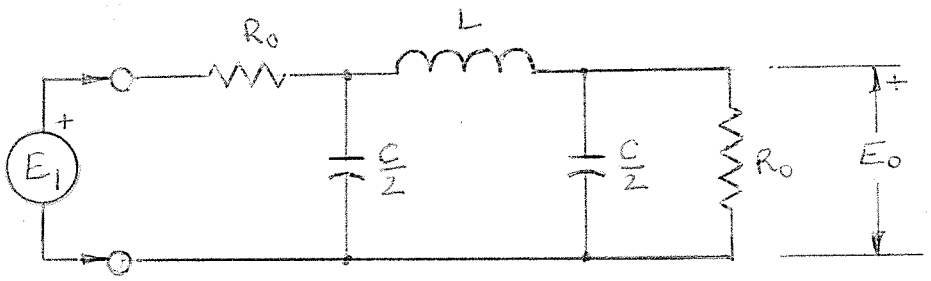

Fig. 23 Constant - k π - section

The analysis shows that the transfer voltage ratio is given by

$$\frac{E_o}{E_1} = \frac{1}{2\left[1 + \left(\frac{L}{2R_o} + \frac{R_oC}{2}\right)S + \frac{LC}{2}S^2 + \frac{R_oC^2}{8}S^3\right]} \qquad (5)$$

Substituting for L and C from equations (3) and (4) this becomes

$$\frac{E_o}{E_1} = \frac{1}{2\left[1 + 2\left(\frac{S}{B}\right) + 2\left(\frac{S}{B}\right)^2 + \left(\frac{S}{B}\right)^3\right]} \qquad (6)$$

If the gain is normalized to the d-c gain and if frequency is normalized to the bandwidth, then

$$\frac{E_o}{E_1} = \frac{1}{1 + 2S + 2S^2 + S^3} \qquad (7)$$

This shows that the constant - k section is also maximally flat.

Factoring (7) we get

$$\frac{E_o}{E_i} = \frac{1}{(S \neq 1)\ (S^2 \neq S \neq 1)} \qquad (8)$$

The asymptotic $\propto$ - diagram (Fig.26) ie. the gain function plotted on a db-log frequency scale gives much information about the cutoff characteristic. There is a linear factor which has a cutoff slope of - 1 and a break frequency of 1, and a quadratic factor which contributes a cutoff slope of -2 and also has a break frequency of 1. The quadratic factor has a damping ratio of $\frac{1}{2}$ and hence the filter characteristic becomes flatter inside the pass-band than it would be if the quadratic were replaced by a squared linear term.

The overall cutoff slope is -3 ie. 60 db per decade as required. For real frequencies equation (7) becomes

$$\frac{E_o}{E_i} = \frac{1}{(1 - 2w^2) \neq j(2w - w^3)} \qquad (9)$$

For $w = \frac{1}{2}$ ie. $f = 80$ cps. $\frac{E_o}{E_i} = .9925$

Thus the filter is flat within $\frac{3}{4}\%$ up to 80 cps, which appears to be excellent.

In order to get comparable performance from an R-C filter four L-sections would be required. To minimize loading the sections would have to be either isolated by isolating amplifiers or their

impedance levels would have to be increased progressively by factors of 10 from the input to the output end.

2. THE DIFFERENTIATOR

The design objectives in the case of the differentiator are good stability and correct scale factor. The basic circuit of a differentiator using an operational amplifier is given in Fig. 24.

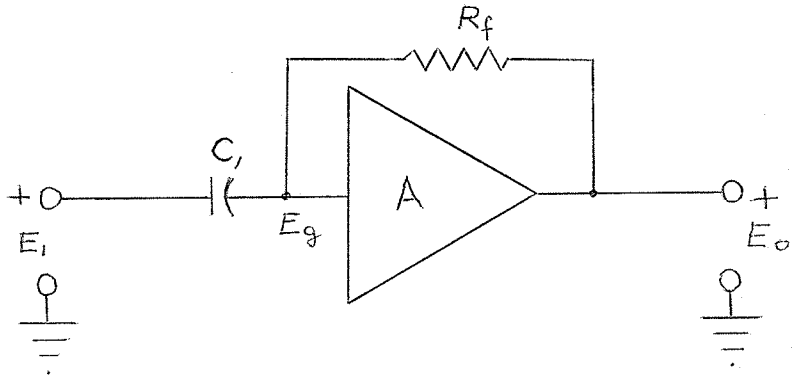

Fig. 24 Basic Differentiator Circuit

The exact transfer functions of this circuit, assuming the operational amplifier to be ideal, is

$$\frac{E_o}{E_1}(S) = \frac{R_f C_1 S}{\frac{R_f C_1}{A} S - 1 + \frac{1}{A}} \qquad (10)$$

A will be much greater than 1, so we can neglect $\frac{1}{A}$ with respect to 1 and write:

$$\frac{E_o}{E_1}(S) = A \frac{S}{S - \frac{A}{R_f C_1}} \qquad (11)$$

A has to be negative ie. the amplifier has to be inverting, otherwise

the transfer function would have a pole in the right-hand plane. For small S the transfer function is $-R_f C_1 s$ while for large S it is A. This means that for frequencies low compared to $\frac{A}{R_f C_1}$ the circuit acts as a differentiator. Also the scale factor of the circuit is RC. From Fig. 6 in Chapter I it is estimated that the maximum rate of change of the signal presented to the differentiator would be $\pm$ 1000 volts per second. If the maximum output voltage swing of which the differentiator is capable is $\pm$ 50 volts, then RC must have the value .05 seconds. This time constant could be made up of C = .1μf and R = 500 k, which are convenient values.

It was found that the basic differentiator amplifies frequencies as high as, or higher than, $\frac{A}{RC}$ radians per second by the factor A. This is undesirable because high-frequency noise is amplified and instability could occur due to phase shifts in the amplifier. Assuming an amplifier gain of 10^4, the quantity $\frac{A}{RC}$ becomes 2×10^5 radians per second or approximately 30 kcps. The highest signal frequencies that the differentiator may be called upon to differentiate accurately are estimated at about 50 cps. The circuit shown in Fig. 25 is arranged to obtain a cutoff of the differentiator response at about 300 cps.

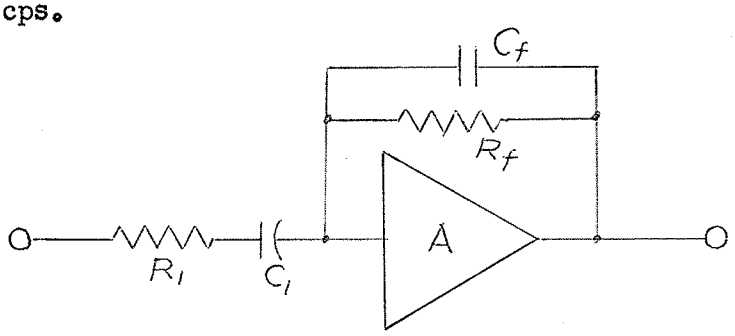

Fig. 25 Stabilized Differentiator

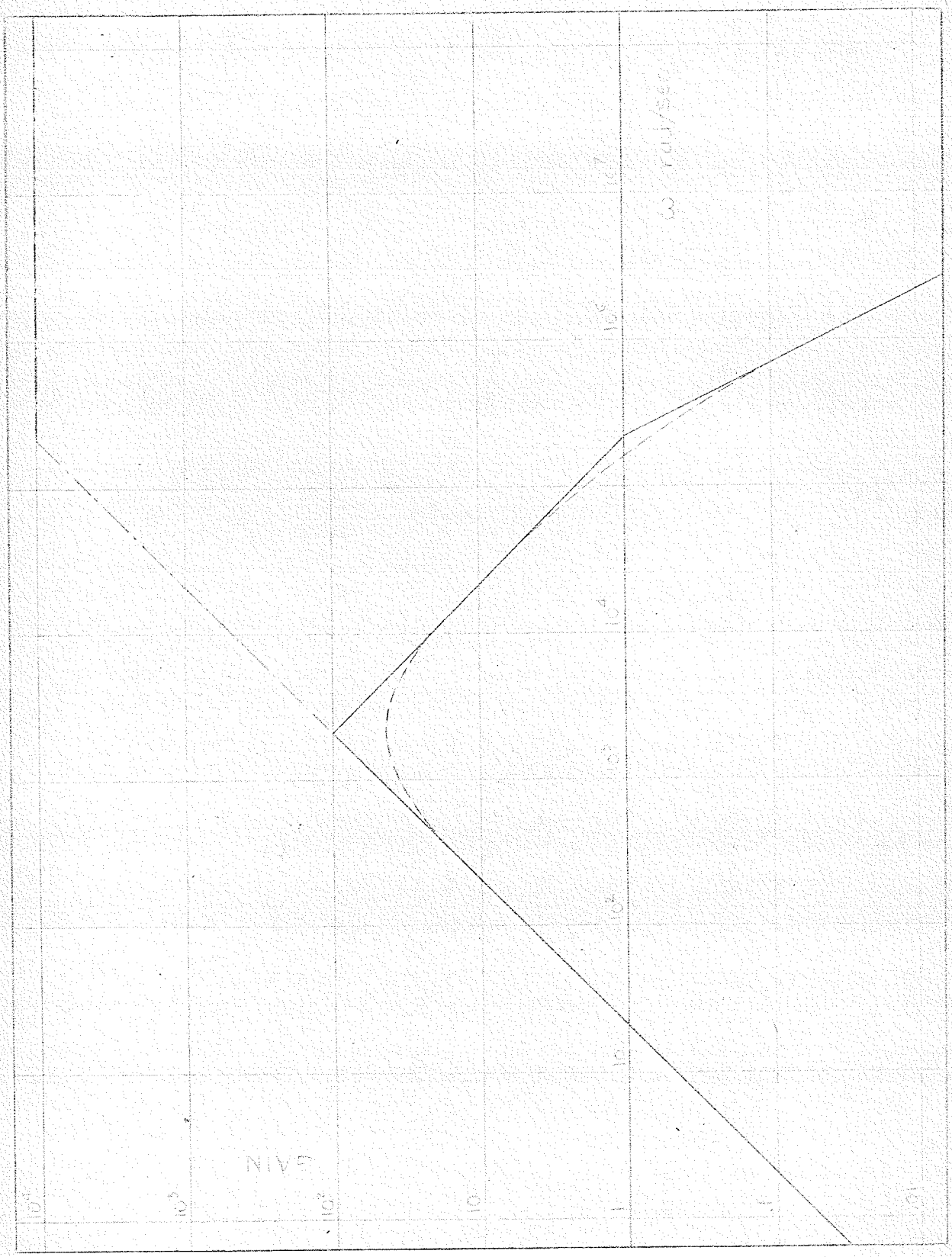

FIG. 2.2 ASYMPTOTIC X-DIAGRAM OF DIFFERENTIATED FISSION NEUTRONS.

The transfer function of this circuit, assuming that the amplifier is ideal and has a gain which approaches infinity, is given by

$$\frac{E_o}{E_i} = \frac{- sR_fC_i}{(1 + sR_f C_f)\ (1 + sR_iC_i)} \qquad (12)$$

The break frequencies corresponding to the two linear terms in the denominator are to be at 300 cps or 2×10^3 radians per second. Hence $R_f C_f = R_iC_i = 5 \times 10^{-4}$ sec. Since R_f and C_i have been chosen already, R_i and C_f must have the values 5 k and .001 μf respectively.

The complete asymptotic diagram of the resultant differentiator response isshown in Fig. 26. The dot-dashed line is the response of the basic differentiator circuit. The dotted curves represent the actual response curve in the regions where it differs appreciably from the asymptotic response. The diagram indicates that the differentiation should be accurate for frequency components up to about 600 rad/sec or 100 cps.

To get a better estimate of the expected accuracy of the differentiator, suppose that during a complete σ-sweep the output of the central unit is a ramp function. The exact differentiation would produce a step function whose height is equal to the slope of the ramp.

The Laplace Transform of the ramp is $\frac{1}{S^2}$ and $E_o(S)$ becomes

$$E_o(s) = \frac{-.05}{S(1 + 5 \times 10^{-4} S)^2} \qquad (13)$$

The inverse transform of (13) is

$$e_o(t) = -T^2 \left[(1 - e^{-\frac{t}{T}}) - \frac{t}{T} e^{-\frac{t}{T}} \right]$$

where $T = 5 \times 10^{-4}$ sec. A plot of this function is shown in Fig. 27

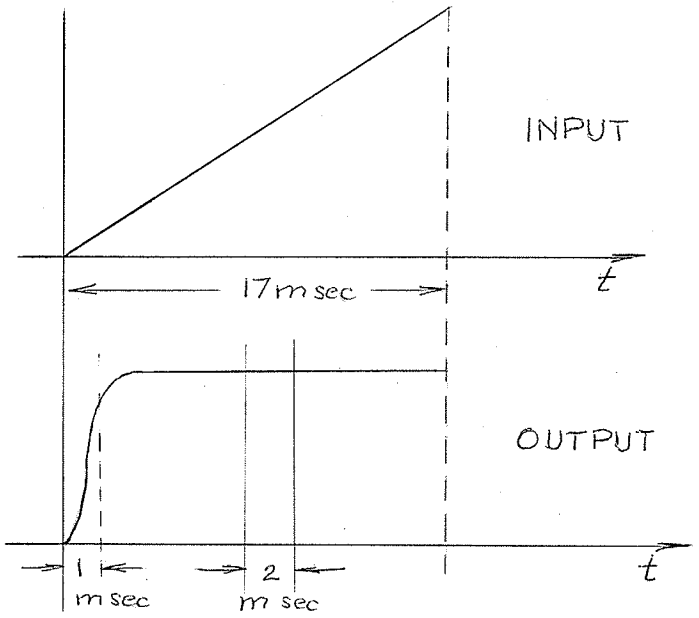

Fig. 27 Differentiator response to a ramp

The output of the differentiator reaches practically 100% of the slope of the ramp long before the sampling interval.

The response to an input which is a segment of a parabola is the time integral of the response to the ramp, and is shown in

Fig. 28.

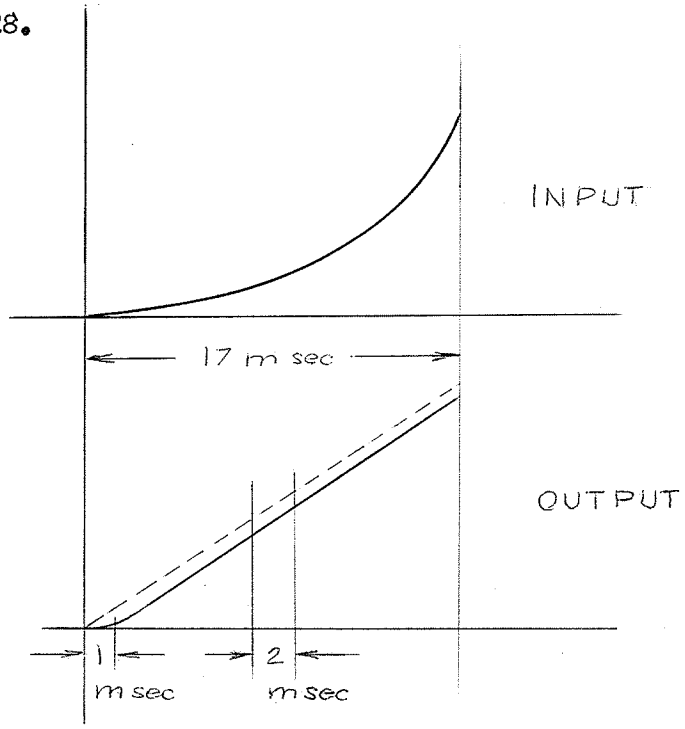

Fig. 28 Differentiator response to a parabola

In both cases the signal is delayed by 1 msec, and the resulting error at the sampling interval depends on the rate of change of slope of the input function. This delay can easily be compensated for by delaying the sampling interval by 1 msec also.

3. THE GATE

A six-diode gate is used to connect the output of the differentiator to the hold capacitor. When open, the gate has a back resistance of a single diode, and when closed, the forward resistance of one diode.

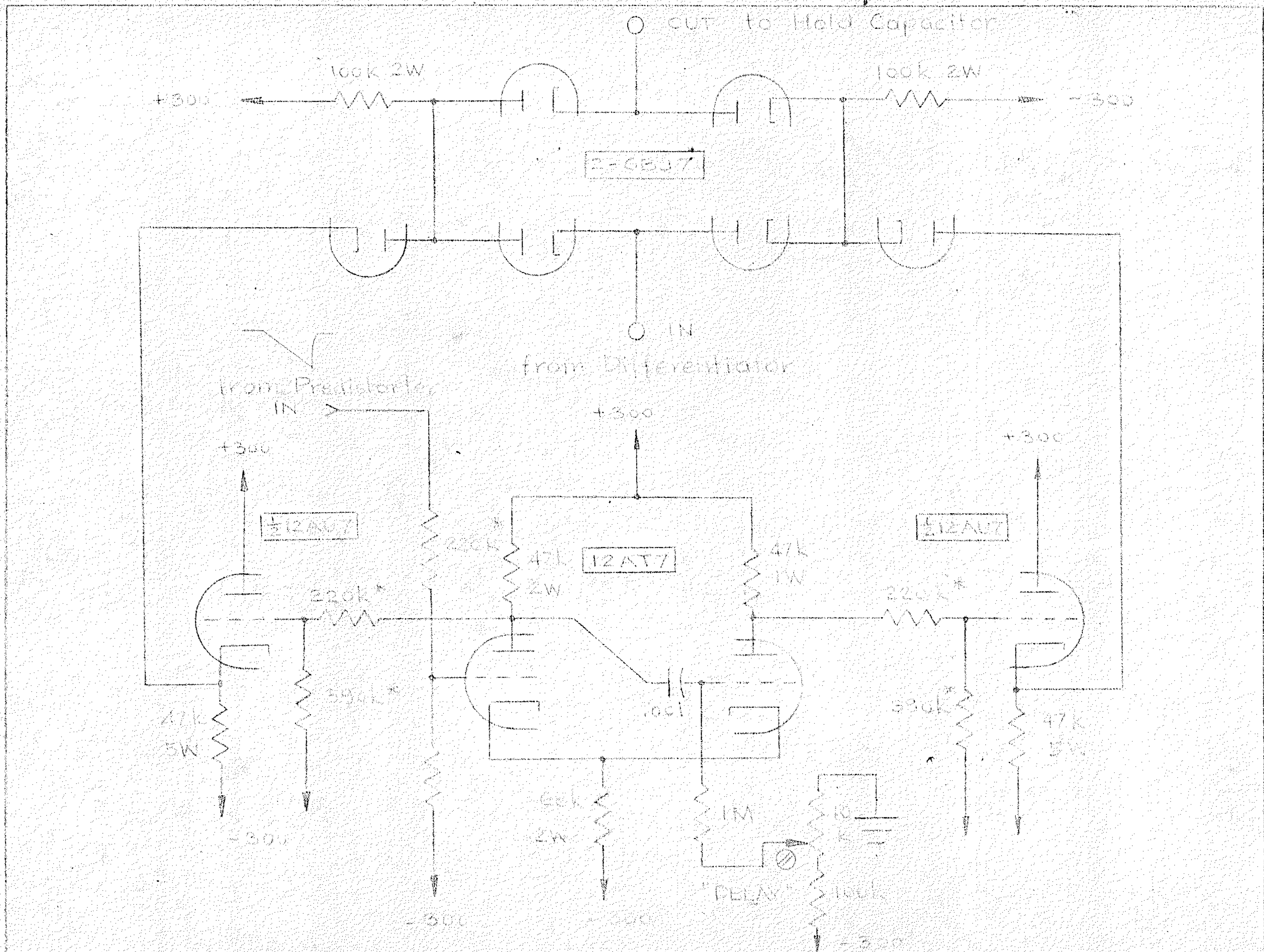

FIG. 29 SIX-DIODE GATE, GATE DRIVER, DELAY MULTI

The circuit diagram is shown in Fig. 29. The six-diode gate is a high-precision device and can be regarded as a practically perfect switch. (Mi 2)

The gate has been set up such that in the closed state, with no input, each diode conducts 1.5 mA. This allows a maximum signal current of 3 mA through the gate, because there are 2 parallel paths. A control voltage swing of ± 55 volts is used, so that a maximum signal voltage swing of ± 50 volts is permissible. The control current in the open condition amounts to 3.5 mA.

4. GATE DRIVER AND DELAY MULTIVIBRATOR

A 12AU7 is used in cathode follower connection to supply the control voltages of ± 55 volts at a current of 3.5 mA to the gate. (Fig. 29) The d-c level of the pulses appearing at the plates of the delay monostable multivibrator is about + 200 volts, but the d-c level of the control pulses must be zero. Resistive coupling from the plates of the multivibrator to the grids of the cathode followers is used to lower the d-c level.

The input to the delay multivibrator is taken from the plate of the predistortor, where the sawtooth is negative-going and has an amplitude of about 40 volts peak-to-peak. Its d-c level also has to be adjusted until the sawtooth signal is always negative at the grid of the multivibrator, but this is not critical. The time delay

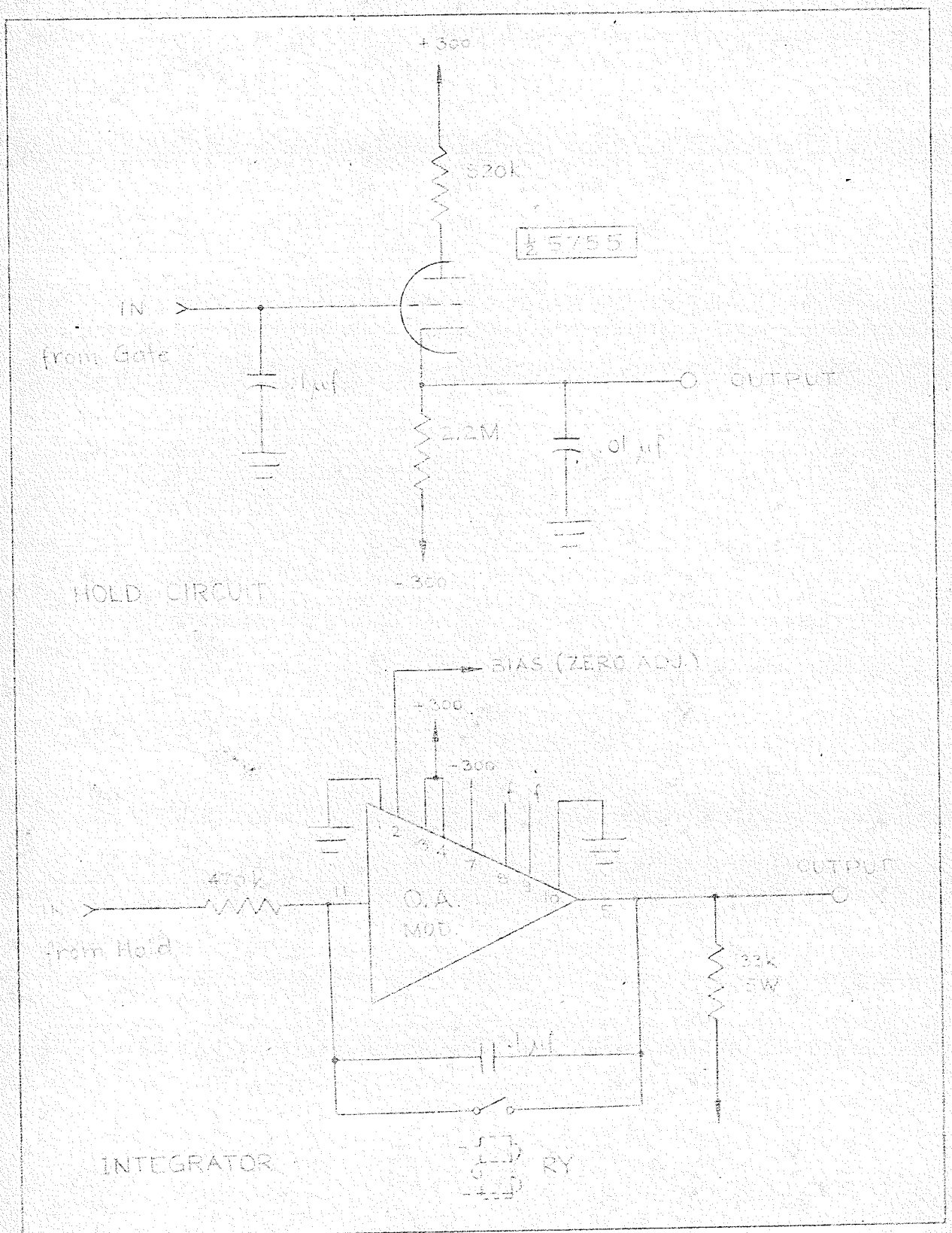

FIG. 30 HOLD CIRCUIT AND INTEGRATOR

can be adjusted by the 10k potentiometer so that the gate closes exactly at the time when the σ-sweep crosses the jw-axis.

The adjustment can be performed with the help of an oscilloscope having a differential input or a double-beam oscilloscope. The σ-sweep waveform is connected to the A input and the pulses from the multivibrator to the B input. If the selector switch is set to A - B, then the two waveforms will appear superimposed on each other on the screen of the oscilloscope, and the coincidence can be set. The gate duration can be adjusted to 2 msec by selecting the values of the .001 μf capacitor and the 1M resistor.

5. THE HOLD CIRCUIT

The hold circuit consists simply of a capacitor and a special cathode follower designed for very low grid current. When the gate closes, the capacitor is connected to the output of the differentiator, and it holds the charge until the next sample is taken. To calculate the maximum permissible value of the hold capacitor it is assumed that the maximum voltage change from one sample to the next is 20 V. Such large and fast voltage charges are limited by the current capacity of the gate, which is 3 mA. Substituting in the formula

$$i = C \frac{de}{dt}$$

the values $i = 3 \times 10^{-3}$ amperes and $\frac{de}{dt} = 10^3$ volts per second and

solving for C we get

$$C_{max} = .3\ \mu f$$

A .1 μf capacitor would be entirely adequate, because the duration of the hold is only 20 msec. If it is assumed that the back resistance of the diodes and the input impedance of hold cathode follower are in excess of 100 megohms, then the time constant of the hold is greater than 10 seconds. The initial fall of the capacitor voltage is 10% per second, .2% during the active hold period of 20 msec.

When the voltage change from one sample to the next is less than .75 volt then the capacitor charges in 25 μsec, which is very fast.

The diagram of the hold circuit is shown in Fig. 30.

6. THE INTEGRATOR

The integrator is very similar to the one used in the staircase function generator of the input unit (Fig. 30). The initial condition relay for this integrator can be the same one which is used in the staircase function generator, but that relay will have to be changed from a DPDT type to a 3PDT type.

B I B L I O G R A P H Y

Bi 1 S. Bigelow, and J. Wuorinen, "An Extended Angular Range Direct Reading Phasemeter", Columbia University - Electronics Res. Lab. Report; September 20, 1956.

Bk 1 H. W. Bode, Network Analysis and Feedback Amplifier Design D. Van Nostrand 1945

Ch 1 R. V. Churchill, Introduction to Complex Variables and Applications, McGraw-Hill Book Company, Inc., New York, N. Y.; 1948

Gu 1 Guillemin E.A., Introductory Circuit Theory Wiley 1953

Ko 1 G. A. Korn, and T. M. Korn, Electronic Analog Computers, Second Edition, McGraw-Hill Book Company, Inc., New York, N. J.; 1956

Kr 1 G. Kranc, P. Mauzey, and J. Wuorinen, "Complex Plane Scanner - An Analog Computer", Columbia University - Electronics Res. Lab. Report; August 1, 1955.

Mi 1 Millman & Taub, Pulse and Digital Circuits, McGraw-Hill Book Company, Inc., New York, N. Y.; 1956

Mi 2 J. Millman & T. H. Puckett, "Accurate Linear Bidirectional Diode Gates", Proc. I.R.E., Vol. 43, No. 1, pp. 29-38, January 1955.

Se 1 S. Seely, Electronic Engineering, McGraw-Hill Book Company, Inc., New York, N. Y.; 1956

St 1 J. L. Stewart, Circuit Theory and Design, John Wiley and Sons Inc., New York, N. Y.; 1956

Va 1 Valley and Wallman, Vacuum Tube Amplifiers, McGraw-Hill Book Company, Inc., New York, N. Y.; 1958 (M.I.T., Radiation Laboratory Series, Vol. 18)

Va 2 E. P. Valstyn, "A Complex-Plane Scanner", M.Sc. Thesis, University of Manitoba, October 1958

APPENDIX

ANALYSIS OF THE EQUIVALENT EDISON GENERATOR

Waveform at the output of the sawtooth generator:

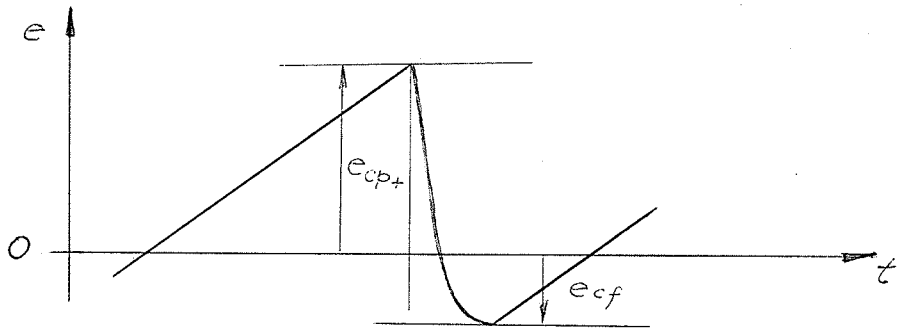

e_{cp+} is the positive peak value of the sawtooth;

e_{cf} is the final value of the voltage across the capacitor C after the discharge.

The equivalent circuit of the sawtooth generator during the discharge is assumed to be as follows:

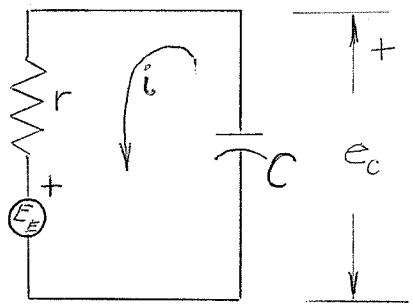

The tube is represented by the Edison Generator in series with the beam resistance r.

The equations governing this circuit are:

$$E_E + ri = e_c \qquad \text{- - - - (1)}$$

$$i = -C \frac{de_c}{dt} \qquad \text{- - - - (2)}$$

Substituting from (2) in (1), we get

$$rC \frac{de_c}{dt} + e_c = E_E \qquad \text{- - - - (3)}$$

Taking the Laplace Transform, we have

$$rC\,(sE_c - e_{cp+}) + E_c = \frac{E_E}{s} \qquad \text{- - - - (4)}$$

where the inital voltage across the capacitor, e_{cp+}, was substituted.

Solving for E_c

$$E_c\,(s) = \frac{\frac{E_E}{s} + rCe_{cp+}}{rCs + 1} \qquad \text{- - - - (5)}$$

$$\text{or} \quad E_c\,(s) = \frac{e_{cp+}}{s + 1/rC} + \frac{E_E/rC}{s(s + 1/rC)}$$

Taking the Inverse Laplace Transform, we get

$$e_c(t) = E_E + (e_{cp+} - E_E)e^{-\frac{t}{RC}} \qquad \text{- - - - (6)}$$

From this we can calculate the initial slope of the discharge curve

$$\left.\frac{de_c}{dt}\right]_{t=o} = \left.\frac{(e_{cp+} - E_E)e^{\frac{-t}{RC}}}{-rC}\right]_{t=o} = \frac{E_E - e_{cp+}}{rC} \qquad \text{- - -(7)}$$

We can also calculate the time at which the discharge curve crosses the time-axis.

$$t = rC \ln\left(1 - \frac{e_{cp+}}{E_E}\right) \qquad \text{- - - - - (8)}$$

The inital slope was measured at 10^4 V/sec, e_{cp+} was measured at 2.5V, and t was measured to be .58 msec.

Substituting these data in equations (7) and (8) we can calculate r and E_E.

We find $r = 290$ ohms and

$$E_E = -.4 \text{ volt}$$

These figures appear to be inaccurate, because from the shape of the discharge curve it can be inferred that the total discharge time is at least 3 times as long as the discharge time constant.

Hence E_E should be equal to -1.5 volts, because the capacitor would finally charge to the voltage of the Edison Generator.

Using this value of E_E and the data on initial slope, we get $r = 400$ ohms and using $E_E = -1.5$ V and the time of zero crossover, we get $r = 580$ ohms. The discrepancy must be due to errors in the measurement of the slope and crossover.

Finally the most probable values of E_E and r are estimated to be

$E_E = -1.5$ volts

$r = 500$ ohms